UNIVERSITÀ DEGLI STUDI
DI MILANO

DOTTORATO IN MEDICINA MOLECOLARE E TRASLAZIONALE

CICLO XXXII
Anno Accademico 2018/2019

TESI DI DOTTORATO DI RICERCA

MED/08

Further insight into V-ATPase role in glioma stem cells

Dottorando: Alessandra Maria Storaci
Matricola N°: R11530

TUTORE: Prof. Stefano Ferrero
CO-TUTORE: Dott.ssa Valentina Vaira

COORDINATORE DEL DOTTORATO: Prof. Michele SAMAJA

ABSTRACT

V-ATPase is a proton pump mainly localized on lysosomes and on plasma membrane of specialized cells. It is responsible of proton translocation and acidification of intra- and extra-cellular environment.

Our group demonstrated that the over-expression of the subunit G1 (V1G1) is involved in the maintenance of the stem cell niche in glioblastoma (GBM) and correlates with poor prognosis in GBM patients.

In this work we aimed to elucidate the role of V-ATPase in GBM stem cells from a functional perspective.

We demonstrated that neurospheres (NS) with higher levels of V1G1 subunit (High-V1G1), compared with NS with lower levels of V1G1 (Low-V1G1), were characterized by increased clonogenicity in vitro and in vivo, invasiveness, lysosomal acidification and ERK pathway activation. Specific inhibition of V-ATPase activity, by Bafilomycin (BafA1), but not of ERK or other lysosomal drugs, induced reactive oxygen species (ROS)-mediated apoptosis only in High-V1G1 NS. In addition, BafA1 treatment affected mitochondria homeostasis only in High-V1G1 NS. Preliminary experiments suggested that a V-ATPase pump might be localized on the mitochondria or it could mediate direct contacts between mitochondria and lysosomes thus causing an imbalance of charges (proton flux) when perturbed.

Finally, High-V1G1 and Low-V1G1 NS differed in terms of metabolic behaviours: preferential use of glycolysis by Low-V1G1 NS opposite to use of oxidative metabolism in High-V1G1 NS. V-ATPase block by BafA1 in High-V1G1 NS shifted their metabolism to that of Low-V1G1 NS. On the other hand, the autophagic pathway, that is directly connected with lysosomal function, was blocked by BafA1 only in Low-V1G1 NS. These phenotypes were not modulated by ERK or lysosomal acidification inhibitors alone, indicating a specific role for V-ATPase proton pump in modulating them.

Taken together, these results indicate that V-ATPase is crucial for GBM stem cells viability through different mechanisms that include bioenergetics sensing and requiring, mitochondrial homeostasis and ERK signalling activity.

SOMMARIO

La V-ATPasi è una pompa protonica localizzata principalmente sui lisosomi e sulla membrana plasmatica di cellule specializzate. È responsabile della traslocazione dei protoni e dell'acidificazione dell'ambiente intra ed extra cellulare.

Il nostro gruppo ha dimostrato che un'alta espressione della subunità G1 (V1G1) influisce sul mantenimento della nicchia staminale nel glioblastoma (GBM) e correla con una prognosi sfavorevole nei pazienti con GBM.

Lo scopo di questo lavoro mira a chiarire il ruolo della V-ATPasi nelle cellule staminali di GBM a livello funzionale.

Abbiamo dimostrato che neurosfere (NS) con alti livelli della subunità G1 (High-V1G1), paragonate con NS con bassi livelli di V1G1 (Low-V1G1), sono caratterizzate da un maggiore potenziale clonogenico, in vitro e in vivo, da una maggiore capacità di invadere, da lisosomi più acidi e da una maggiore attivazione del pathway di ERK.

L'inibizione specifica dell'attività della V-ATPasi da parte della BafilomicinaA1 (BafA1) induce attivazione dell'apoptosi mediata dalla presenza delle specie reattive dell'ossigeno (ROS) nelle NS High-V1G1; effetto che non avviene dopo l'inibizione del pathway di ERK o con farmaci contro l'attività del lisosoma.

Il trattamento con la BafA1 influisce anche sull'omeostasi dei mitocondri nelle NS High-V1G1.

Esperimenti preliminari suggeriscono che la V-ATPasi possa essere localizzata sui mitocondri o possa mediare il contatto diretto tra questi organelli e i lisosomi, causando uno squilibrio delle cariche (flusso protonico) quando è inibita.

Infine, NS High e Low-V1G1 mostrano diversi tipi di metabolismo: le NS Low-V1G1 usano preferenzialmente un metabolismo di tipo glicolitico, mentre le NS High-V1G1 si basano su un metabolismo di tipo ossidativo.

L'inibizione della V-ATPasi, da parte della BafA1, nelle NS High-V1G1, le induce a modificare il proprio metabolismo e a utilizzarne uno simile a quello delle NS Low-V1G1.

L'autofagia, direttamente connessa alla funzionalità dei lisosomi, invece, viene bloccata dal trattamento con la BafA1 solo nelle NS Low-V1G1.

Gli inibitori del pathway di ERK o dei lisosomi non causano lo stesso tipo di effetti: questo indica che la V-ATPasi ricopre un ruolo specifico nella modulazione di questi meccanismi.

Nell'insieme, questi dati indicano che la V-ATPasi ha un ruolo cruciale nel preservare la vitalità delle cellule staminali di GBM attraverso meccanismi che includono la regolazione del metabolismo, l'omeostasi dei mitocondri e l'attività del pathway di ERK.

INDEX

1.INTRODUCTION

1.1. Glioblastoma

Gliomas are central nervous system tumors classified in three groups, astrocytomas, oligodendrogliomas and ependymomas, according to tumor type origin; while their behavior assigns a grade that increases with aggressiveness [1].

Glioblastoma (GBM) is classified as an astrocytomas of IV grade and it represents the most common, aggressive and malignant primary brain tumor in adults with a median survival of 15 months [2–4]. GBM originates *de novo*, without a lower grade precursor (primary GBM) or derives from a lower-grade glioma (secondary GBM) [2].

Both types of GBM can show genetic alteration as mutation of TP53, TERT, IDH1/2, amplification of EGFR or pRB deletion [1].

Diagnosis of GBM is based on the histologic observation of microvascular proliferation and/or necrosis, but, because of cellular heterogeneity, molecular analysis classified GBM in four subtypes: proneural, neural, mesenchymal and classical [2,5].

1.1.1. GBM stem cells

GBM is characterized by cancer cells with elevated heterogenicity and plasticity, high ability to invade and drug treatment resistance, thus disease recurrence is frequent [6–8]. Its aggressive behaviour is also related to the presence of glioma stem cells (GSC), a sub-population of tumor cells that self-renews, proliferates to maintain tumor growth and is able to recapitulate tumor characteristics if injected in mice (Fig1) [9,10].

GSC are sourronded by a specific micro-environment characterized by the release of factors and by cells interactions that maintain GSC population [10]. Stem cell niche shows high grade of hypoxia that induces GSC to secrete molecules responsible of vassels remodeling; moreover GSCs are able to differentiate in perycites or endothelial-like cells, forming blood-tumor barrier [11].

GBM cells, promoting the formation of a stiff extracellular matrix characterized by the high level of glycoproteins, support proliferation and invasiveness of GSC by the activation of integrin-notch pathway [12].

Also immune system is involved in the regulation of stem cell niche, in particular Tumor Associated Macrophages (TAM) contribute to GSC stimulation promoting glycolitic metabolism [13,14].

On the other hand GSC modulate innate immune system to avoid tumor suppression, down-regulating immune cell receptors [15].

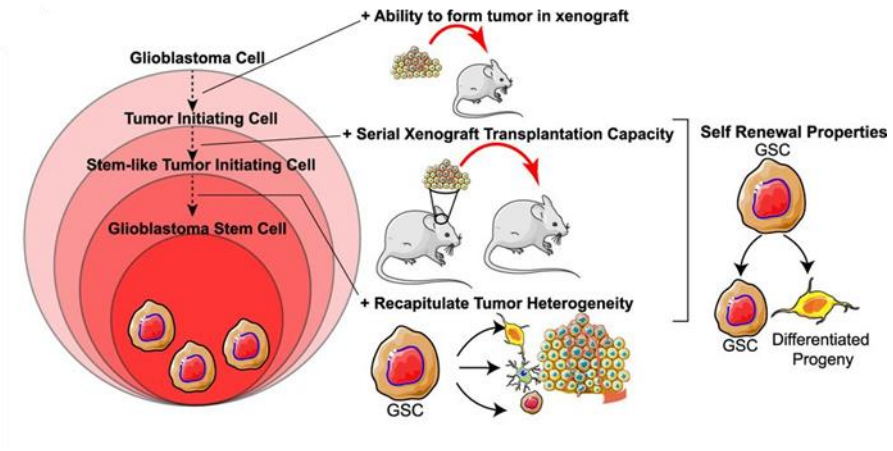

Fig1. Cancer stem cells characteristics.
From Gimple et al. 2019 “Glioblastoma stem cells: lessons from the tumor hierarchy in a lethal cancer”. Genes Dev

1.1.2. GBM therapy strategies

Due to the high heterogenity and unique microenvironment the main treatment for GBM is surgical resection followed by radiotherapy [16]. The only approved therapheutic agents for this type of cancer are: temozolomide (TMZ) for newly diagnosed GBM and the anti-VEGF, bevacizumab, for recurrent GBM [17,18].

Despite the therapeutic limitations given by the heterogenic cell population, the presence of compensatory pathways that interfere with drugs effects and the limited drug concentration in brain due to blood-brain-barrier, new promising approaches have been developed in the last years [16,19] (Fig2). Among them, targeting immune checkpoint could oppose the immunosoppression activated by the tumor: anti-CTLA4 antibody reduces apoptosis and cell cycle arrest in activated T cell and it decreases regulatory T cell activation, while anti-PD1 antibody increases the number of CD8+ cells, both resulting in anti-tumor effect [20,21].

Other strategies based on immuno modulation involve CAR-T cells, modified to recognize tumor specific antigens (i.e. EGFRvIII, HER2 and IL-13Rα2) and dendritic cells, collected from patients, incubated with tumor antigens or lysate and reinjected [22,23].

Virotherapy, instead, takes advantage of oncolytic or immuno stimulatory viruses that are able to express citotoxic genes or to promote the anti-tumor response, if injected directly in tumor site [24].

Among the therapies developed against GSC, the targeting of telomere-protecting factor (TRF1) and circadian rhythm regulators reduce cell viability [25,26].

All these strategies showed promising data from preclinical trials, but more studies must be carry on to reduce toxicity, advers events, to find new targets and to escape the high genetic heterogenity of GBM that causes therapy resistence [16].

Table 1. Summary of Various Novel Therapeutic Modalities for Glioblastoma

Therapeutic Modality	Mechanism	Targets/Vectors in GBM	Benefits	Drawbacks	U.S. Food and Drug Administration Approvals
Immune checkpoint inhibitors	Antibodies target/block immune checkpoint proteins involved in the inhibition of T cell activation and the activation of regulatory T cells	Cytotoxic T lymphocyte—associated protein 4, programmed cell death protein 1, programmed death-ligand 1, indoleamine-2,3-dioxygenase	Longer response period, lower rate of high-grade toxicities, targeted therapies based on genotyping	Low mutational loads/paucity of GBM-infiltrating T cells, genetic/antigenic heterogeneity of GBM, immunosuppressive GBM microenvironment	Anti—programmed cell death protein 1/programmed death-ligand 1: melanoma (2014), non—small-cell lung cancer (2015), Hodgkin lymphoma, renal cell carcinoma, bladder, head/neck (2016), metastatic Merkel cell carcinoma, stomach, gastroesophageal (2017), liver, squamous cell carcinoma, small-cell lung cancer, colorectal, cervical, kidney (2018) Anti—cytotoxic T-lymphocyte-associated protein 4: late-stage melanoma (2011), renal cell carcinoma, colorectal, kidney (2018)
Chimeric antigen receptor T cells	T cells genetically engineered to produce an artificial T cell receptor	Epidermal growth factor receptor variant III, human epidermal growth factor receptor 2, interleukin 13 receptor subunit α2, mucin 1, isocitrate dehydrogenase 1, survivin	Short treatment time/single infusion, rapid recovery, longer response period "living drug"	Scarcity of GBM tumor antigens, immunosuppressive/nutrient/metabolic suppression of GBM microenvironment, GBM heterogeneity/antigen loss	CD-19: tisagenlecleucel (Kymriah)—relapsed/refractory B cell ALL, axicabtagene ciloleucel (Yescarta)—relapsed/refractory diffuse large C cell lymphoma (2017)
Dendritic cell and vaccination	Dendritic cells harvested from patient, exposed to tumor-specific peptides/tumor lysate and re-injected into patient to generate antigen specific T cell response	Glioblastoma-associated antigens: antigen isolated from immunoselected melanoma 2, interleukin 13 receptor subunit α2 chain, human epidermal growth factor receptor 2, ephrin type A receptor 2, glycoprotein 100, tenascin, surviving, melanoma antigen gene, chitinase-3-like protein, Wilms tumor protein 1, SRY-related HMG-box 11, cytomegalovirus Glioblastoma-specific antigens: epidermal growth factor receptor variant III	Promotes long-term antitumor immune response, lower high-grade toxicity	Low number of DCs in GBM tumor site, poor access of DCs to tumor antigen, limited capacity of tumor cells to activate intratumoral DCs, secretion of cytokines limiting DC maturation	Sipuleucel: metastatic castration-resistant prostate cancer (2010)
Virotherapy	Replication defective: viral replication genes removed, replaced with immune stimulatory/cytotoxic genes Replication selective: viral pathogen engineered with target toward specific tumor cells	Vectors: oncolytic herpes simplex virus 1, Toca511, polio-/rhinovirus (PVSRIPO), oncolytic adenovirus (DNX-2401, tasadenoturev), parvovirus H-1 (ParvOryx)	Well tolerated with few adverse events, production of robust antitumor immune response	Safety issues with uncontrolled delivery of gene into host genome Immune responses to viral therapies may inhibit efficacy	Talimogene laherparepvec: inoperable melanoma lesions (2015)

DC, dendritic cell; GBM, glioblastoma.

Fig2. Novel therapeutic approaches in Glioblastoma.

From Mooney et al. 2019 " Current Approaches and Challenges in the Molecular Therapeutic Targeting of Glioblastoma" . World Neurosurgery

1.2. V-ATPase proton pump

The vacuolar H+ATPase (V-ATPase) is a proton pump ATP dependent with a central role in the acidification of extra- and intra-cellular environment [27]. It is mainly localized on lysosomes, where it is involved in the luminal acidification required for the degradation of cellular material, but it is also present on endosomes, Golgi-derived vesicles and secretory vesicles [28–30]. Moreover, at physiological condition, it could be localized on plasma membrane of specialized cells [31].

1.2.1. V-ATPase structure and mechanism

V-ATPase is a multi-subunit complex composed of two domains: the V1 domain, responsible of ATP hydrolysis, is cytosolic and it is constituted of eight different subunits (A–H); the V0 domain is an integral complex of five different subunits (a, d, c, c′ and c″) and it is responsible of protons translocation (Fig.3) [32].

In both V1 and V0 sectors the different subunits form a ring: in V1 sector A and B subunits, present in 3 copies, compose the catalytic site, while V0 sector is composed of single copies of c’ and c’’ and multiple copies of c forming a proteolipid ring [33].

Subunits D, F and d form a central stalk that connects V0 sector to A_3B_3 complex of V1 sector, while subunits C, E, G, H form three pheripherial stalks. ATP hydrolysis induces the rotation of the central stalk and of the V0 ring, while the peripherial stalks avoid the rotation of A_3B_3 complex.

Rotation facilitates the interaction of a positive charged arginine present on subunit a with negative charged glutamate residues of

V0 subunits that are protonate by H+ entering from cytoplasm. Protons are then released in the luminal compartment with a unidirectional movement [33,34].

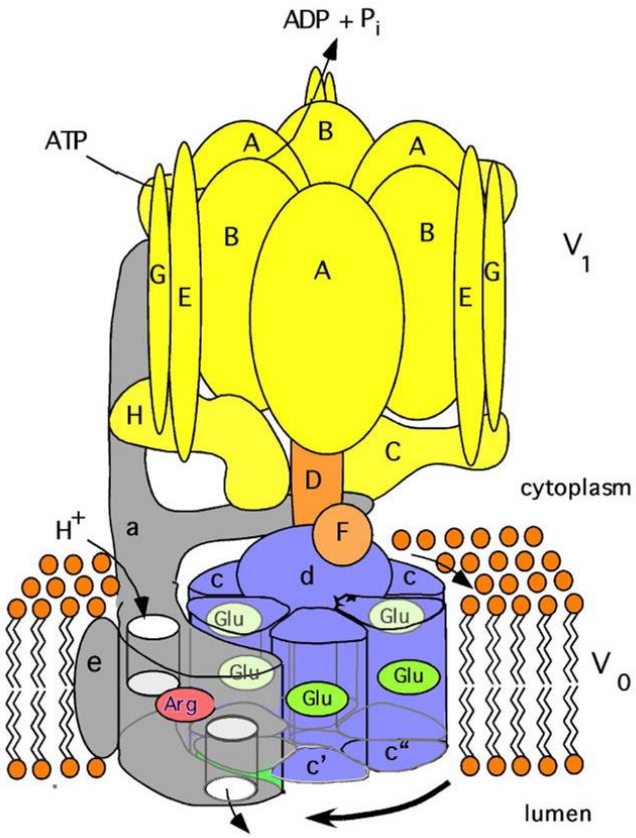

Fig3. Structure of V-ATPase proton pump.
Modified from Toei et al. 2010 “Regulation and Isoform Function of the V-ATPases”. Biochemistry

1.2.2. Bafilomycins

Bafilomycins are a class of macrolide antibiotics, composed by a 16-membered lactone ring and produced by a variety of streptomycetes [35,36]. These antibiotics have different biological activities as antitumoral, antifungal, antiparasitic, immunosoppressant, but moreover, they are specific inhibitors of V-ATPase proton pump by the binding with V0C subunit, preventing proton translocation [35,37–40]. Among Bafilomycins, the A1 (BafA1) is an extremely potent inhibitor of V-ATPase and it was used, together with other proton pump inhibitors as Concanamycin A, to understand consequences of V-ATPase blocking in vitro and in vivo [41,42].

1.2.3. V-ATPase role

V-ATPase plays a key role in different physiological mechanisms based on the acidification of specific cellular compartments [31].

The most known role of V-ATPase is the acidification of intracellular vesicles as endosomes and lysosomes to facilitate endocitosis and to maintain the activity of degradative enzyme respectively [43,44].

Lysosomes are able to degrade matherial internalized by endocytosis or phagocitosis and intracellular substances by autophagy [43].

In endo-lysosomal degradation, extracellular material is internalized and, from plasma membrane, it passes through endosomial intermediates that maturate from early endosomes to late endosomes during autophagy. This process is activated by cell stress, starvation or demaged organelles or cell material that is engulfed in autophagosomes [43,45,46].

In both cases late endosomes and autophagosomes fuse with lysosomes that contains enzymes, like cathepsins and hydrolases, that, thanks to the acidic lumen of the organelle maintained by V-ATPase activity, are able to degrade cell elements [43,46].

In this contest, V-ATPase is implicated in Notch and Wnt signalling, in particular in the endocytosis and processing of Notch and Wnt receptors (respectively NICD and LRP6) by endosomes and lysosomes (Fig4. B and A) [47,48]. Evidences in drosophila and rat indicate that the impairment of V-ATPase affect also the processing of the receptor with an impact on downstream Notch signalling [49,50].

Moreover V-ATPase is directly involved in mTOR pathway: when aminoacids are present at high levels V-ATPase directly interacts with Regulator complex that localizes mTORC1 on lysosomes surface, where it is activated and promotes cell growth (Fig.4C) [28].

On the contrary, when the aminoacids level decreases, the interaction between V-ATPase and Regulator complex increases avoiding the localization of mTORC1 on lysosomes; in cytoplasm it is inactive and allows the transcription factor TFEB to translocate into the nucleus where it activates the expression of autophagy and lysosomes related genes [51].

In addition to his role in endosome and lysosomes V-ATPase proton pump is involved in the formation of synaptic vesicles and in the accumulation of neurotransmitters [52].

Moreover, V-ATPase can be localized also on other organelles as Golgi; even if their relation is not clear, evidences indicate that the

mutation of the a2 subunit correlates with a defect in glycosilation in this organelle [53].

At physiological condition V-ATPase is also present on cell membrane of specialized cells as renal intercalated cells, where it acidificates urine, osteoclasts, where it is involved in bone resorption and clear cells of epididymus, where it contributes to acidify seminal fluid [54–56].

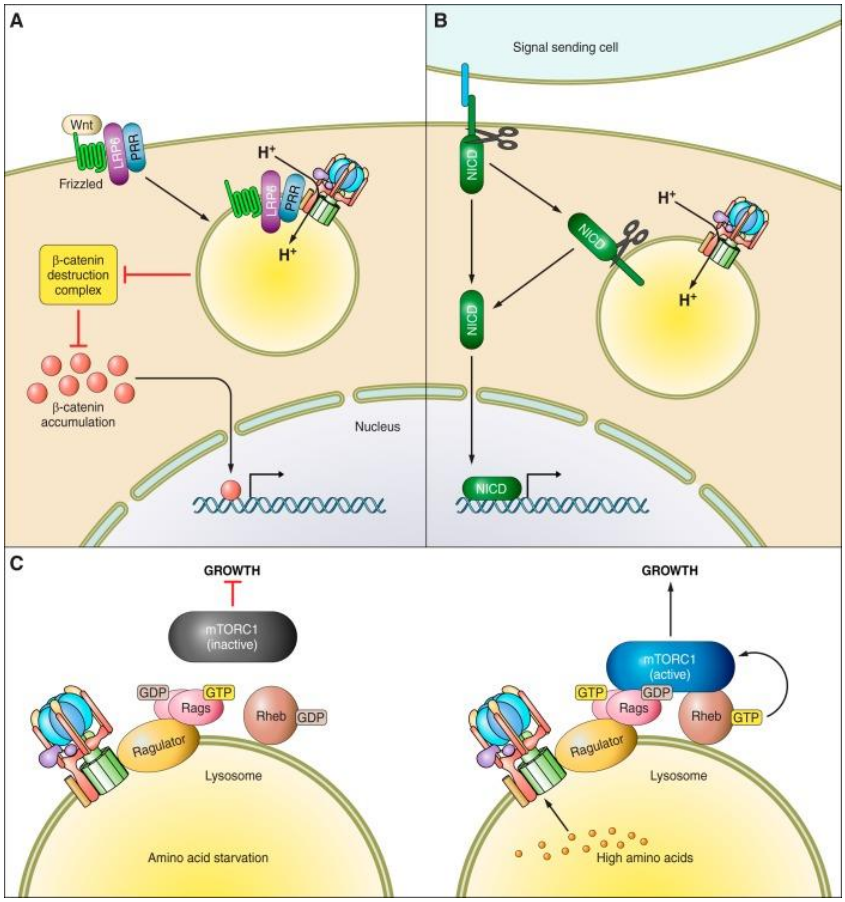

Fig4. V-ATPase and cell signaling.
From Stransky et al. 2016 “The Function of V-ATPases in Cancer”. Physiological Reviews

1.2.4. V-ATPase in cancer

Many evidences in literature demonstrate a deregulation of V-ATPase expression in cancer tissue, in comparison with the normal counterpart [42]. For example, V1C1 subunit expression is associated with a poor prognosis in breast cancer, while V1E1 and V1A are upregulated in esophageal squamous cell carcinoma and gastric cancer respectively [57–59]. These results indicate that the higher expression of V-ATPase in cancer cells favours their survival [28] and many works demonstrate that the proton pump could be localized on plasma membrane of different tumor cells as melanoma, breast, liver, lung, ovarian, prostate and pancreatic cancer [60–68]. This facilitates invasion and migration of cancer cells through many mechanisms: V-ATPase maintains neutral cytosolic pH and acidifys the extracellular environment activating proteases, like cathepsins and metalloproteases, that digest the extracellular matrix; it is also able to interact with actin, inducing a cytoskeleton remodeling; it is involved in the trafficking of pro-invasive factors and it modifies cell membrane potential (Fig.5) [29,60,69]

Moreover it alters chemotherapeutics uptake and efficiency: the acidic extracellular pH modifies drugs charge and prevents their ability to enter the cells or causes their capture in acidic vesicle inside the cell, impairing pharmacological action (Fig.5) [70,71].

The involvement of V-ATPase in cell signaling pathways like Notch, Wnt and mTOR could cause the upregulaton of pro-oncogenic factors that promote cancer cell growth and survival (Fig.5) [28].

V-ATPase activity on lysosomes instead, modulates autophagy that has a role both in tumor suppression and tumor promotion.

Tumor cells could take advantage of autophagy that provides energy by the digestion of cell material; on the other hand a prolonged autophagy could induce cell death (Fig.5) [72,73].

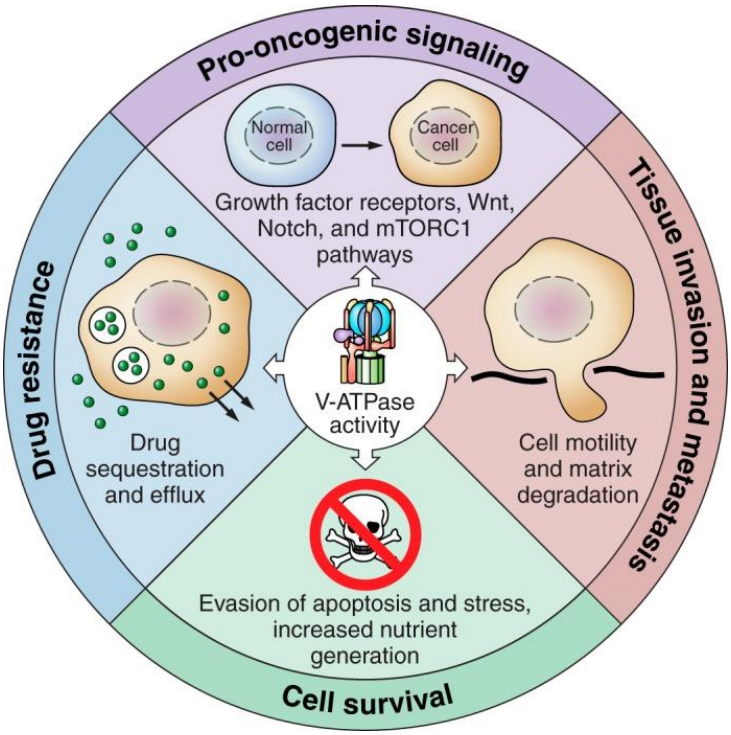

Fig.5 V-ATPase in Cancer cells.
From Stransky et al. 2016 “The Function of V-ATPases in Cancer”. Physiological Reviews.

Different studies indicate that the overexpression of a particular subunit of V-ATPase could promote the localization of the proton pump or the aggressiveness of cancer cell [28].

In our laboratory it was demonstrated that V1G1 subunit is overexpressed in gliomas and expecially it correlates with stemness and aggressiveness while its level decreases during differentiation [27].

The analysis of V-ATPase subunits gene expression from TGCA database, suggests the presence of a specific proton pump configuration that distinguishes low grade gliomas from glioblastoma (GBM), with a higher expression of V1G1 V0A2, V0E1 and V0B in high grade tumours; moreover high level of V1G1 correlates with short survival of patients indicating that it could be a prognostic marker for higher aggressive gliomas [27,74].

In neurosphere (NS) formed by GBM stem cells, directly isolated from patients, it was observed that at basal condition the higher expression of V1G1 subunit correlates with the activation of mTOR and ERK pathways (unpublished data) and that the specific inhibition of V-ATPase by BafilomycinA1 or the reduction of its expression by silencing, reduces lysosomes acidification, spheres area, sphere formation and invasion ability and it decreases cell viability inducing apoptosis [27].

NS are able to produce extracellular vesicles and among them, Large Oncosomes (LO), that originate directly from plasma membrane and bring different signals, as proteins and RNAs, able to modify the microenvironment [75,76].

In our laboratory it was demonstrated that LO isolated from NS are able to reprogram recipient cells and this effect correlates with the ability of vehiculating V1G1 subunit; in particular LO from High-V1G1 NS express higher levels of this proton pump subunit. The co-culture of non-neoplastic cells with LO^{HIGH} increases their proliferation and survival, while Low-V1G1 NS increased their motility and invasion ability after LO^{HIGH} co-culture [75].

This pro-tumorigenic effect is due to the activation of cancer-related pathways by LO in recipient cells, indicating that vesicles bring signals that can alter the transcriptional status of microenvironmental cells [75].

These results indicate the importance of V-ATPAse proton pump role in GBM stem cell maintenance; in particular the involvement of V1G1 subunit in cell mechanisms and in the modification of extracellular environment.

For these reasons it should be important to better elucidate its role in GBM stem cells in terms of viability and pathway regulation.

2. AIM OF WORK

We aimed to elucidate the role of V-ATPase in glioma stem cell niche phenotypes crucial for their mainteinance. To this end, we investigated differences in cellular and metabolic pathways in neurosphere with Low and High levels of V1G1 expression at basal condition and after inhibition of V-ATPase activity to dissect V-ATPase-mediated signaling in glioma stem cells.

3.MATERIAL AND METHODS

3.1. Patients' samples, cell culture and pharmacological treatment

GBM patients' samples were obtained from Neurosurgery Unit of Fondazione IRCCS Ca' Granda Ospedale Maggiore Policlinico.

All patients signed an informed consent and the study was approved by a local Ethic Committee (IRB#275/2013).

GBM samples were dissociated using enzymatic and mechanical method (Tumor dissociation kit, Miltenyi Biotec) and the derived neurospheres (NS) were cultured in Neurocult medium (Stem Cell) supplemented of EGF and FGF (Stem Cell) as described [27]. All experiments were performed on 3 Low-V1G1 and 3 High-V1G1 patients. Neurospheres (NS) were treated for 24, 48 and 72h with BafilomycinA1 (BafA1) 10nM or 20nM (sc-201550, Santa Cruz Biotechnology), with Ammonium Chloride (NH_4Cl 10mM) (A0171, Sigma), with PD98059 (PD) 10µM (P-215, Sigma) and for 24h with ROS inhibitor 100µM (SML0737, Sigma).

3.2. *In vivo* experiments

High and Low-V1G1 NS, stably transduced with a luciferase construct, were disaggregated, cells were counted, resuspended in PBS and $1x10^5$ cells were stereotaxically injected in NOD/SCID mice (7–8 weeks of age, Envigo) as described in Terrasi et al., 2019 [74].

Bioluminescence signals were acquired every week, for 109 days, with IVIS SPECTRUM/CT (Perkin Elmer) after intraperitoneally injection of luciferin (150 mg/kg). Animal experiments were carried out in compliance with the institutional guidelines for the care and

use of experimental animals (European Directive 2010/63/UE and the Italian law 26/2014), authorized by the Italian Ministry of Health and approved by the Animal Use and Care Committee of the University of Milan.

3.2.1. Immunoistochemistry

After 109 days from cells injection, mice were sacrificed and brains were formalin fixed and paraffin embedded. 4µm sections were incubated at 37°C for 24h and then with Ki67 primary antibody (1:500 Abcam) for 1h at room temperature.

The detection of primary antibody was performed by a kit using peroxidasediaminobenzidine as the chromogen (Vector DAB Kit).

3.3. Protein analysis

3.3.1. Total protein extraction

Total protein extract were collected incubating NS pellets with lysis buffer (Tris-HCl 50 mM, NaCl 137 mM, Triton X-100 1%, SDS 0,1% protease and phosphatase inhibitors, Roche) overnight at +4°; NS were then sonicated (5 cycles: 30 sec on, 30 sec off, 160W) by Bioruptor (Diagenode) and centrifuged for 15 min at 15000 rcf. Supernatants were collected for further analysis.

3.3.2. Mitochondria isolation

Mitochondria were isolated using Mitochondria Isolation kit for cultured cells (Option B, Thermo Scientific). Briefly, NS were disaggregated by pipetting and 3-7x10^6 cells were homogenized in reagent A by Dounce Tissue Grinder (Fisher Scientific). To check cell lysis efficiency without organelles disruption, different numbers of strokes were tested (Fig.6). For disaggregated NS, 90 strokes were settled as optimal. Cell homogenate was resuspended in reagent C and centrifuged twice at 700 rcf for 10 min 4°C. Supernatant was transferred and centrifuged at 2500 rcf for 15 min 4°C. Supernatant represented the cytosolic fraction, while pellet, that contained mitochondria, was washed with reagent C, then resuspended in TBS Chaps 2% and vortexed to obtain mitochondrial proteins. Reagents and TBS chaps 2% contained protease inhibitor EDTA free (Roche).

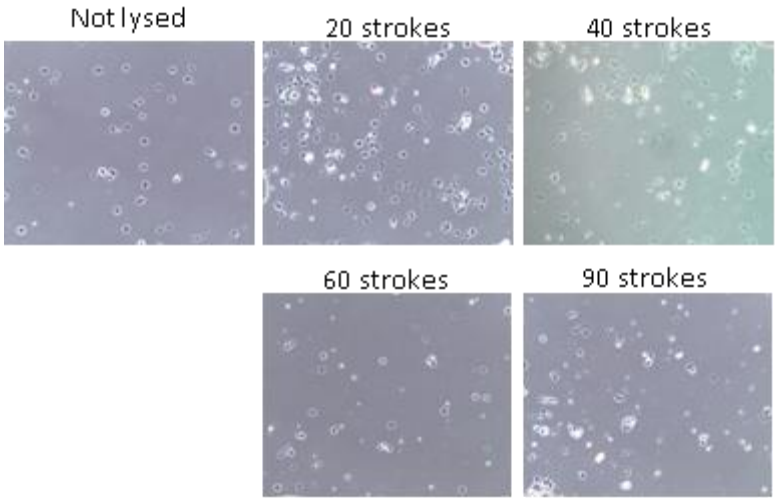

Fig.6: Optimization of cell homogenization protocol
Disaggregated NS were homogenized by a cell douncer and 90 was defined as the optimal number of strokes to disrupt plasma membrane, but not the organelles. Images were obtained by leica DMI6000B microscope.

3.3.3. Protein quantification

Total and mitochondria proteins were quantified by Micro-BCA (Thermo Fisher Scientific), using 1µl of protein extract diluted in PBS and combined to 150µl of Micro-BCA reagents. Absorbance (570 nm) were measured by SAFAS spectrophotometer and unknown samples were compared to BSA standards (Thermo Fisher Scientific).

3.3.4. Western blot analysis

For western blot (WB), 40µg of total protein and 10-20 ug of mitochondria proteins were loaded on 12% acrylamide/bis-acrylamide gel (37:1, Sigma) and transferred on nitrocellulose membranes (BioRad) that were blocked with 5% skim powder milk (70166, Sigma). Membranes were incubated overnight at 4°C with the following primary antibodies: anti-LDHA (1:1000 Cell Signaling Technology), anti-LDHB (1:500 Abcam), anti-MCT1 (1:500 Abcam), anti-GLUT1 (1:1000 Cell Signaling Technology), anti-p62 (1:200, Santa Cruz Biotechnology), anti-ERK (1:1000 Cell Signaling Technology), anti-pERK (1:1000 Cell Signaling Technology), anti-mTOR (1:1000 Cell Signaling Technology), anti-pmTOR (1:1000 Cell Signaling Technology), anti-AKT (1:500 Cell Signaling Technology), anti-pAKT (1:500 Cell Signaling Technology), anti-VDAC (1:1000 Cell Signaling Technology), anti-COX IV (1:1000 Cell Signaling Technology), anti-SDHA (1:1000 Cell Signaling Technology), anti-pyruvate dehydrogenase (1:1000 Cell Signaling Technology), anti-EEA1 (1:1000 Cell Signaling Technology) and anti-cathepsin S (1:500 Abcam).

Anti-βActin (1:1000, Sigma), anti-vinculin (1:1000 Sigma), and anti-βtubulin (1:1000 Sigma) were used as normalizers.
After primary antibody, membranes were incubated with secondary antibody anti-mouse and anti-rabbit (1:5000, BioRad) for 1h at room temperature. Chemiluminescence signals were revealed by ECL (GE Healthcare) and iBright Western Blot Imaging Systems (Thermo Fisher) and quantified by ImageJ software (https://imagej.net).

3.3.5. Phospho Array

Phospho-MAPK-Array (R&D Systems) allows to detect the relative phosphorylation level of 26 kinases. The assay membranes were incubated with 400µg of total proteins and Detection Antibody Cocktail overnight at 4°C. The following day membranes were incubated with Streptavidin-HRP, washed and array spots were detected by iBright Western Blot Imaging Systems (Thermo Fisher) and quantified by ImageJ software (https://imagej.net).

3.4. Electron Microscopy

NS were fixed in 2.5% glutaraldehyde, embedded in 2% agar solution, post-fixed in 1% osmium tetroxide in phosphate buffer, dehydrated and embedded in epoxy resin. Images were captured at 1840X magnification, using a FEI Tecnai G2 20 Transmission Electron Microscope at Alembic – San Raffaele.

3.5. Fluorescence experiments

3.5.1. Immunofluorescence

For immunofluorescence analysis, NS were cytospinned for 3 min at 800 rpm on a microscope slide, fixed for 30 min in PFA 4%, incubated with glycine 20mM for 20 min (to quench green auto-fluorescence) and permeabilized with PBS-Triton 0.5% for 30 min. Blocking was performed by BSA 10% PBS-Triton 0.1% for 1 h at room temperature and then NS were incubated overnight at 4°C with anti-p62 (1:50, Santa Cruz biotechnology) and with secondary antibody (1:1000) 1h at room temperature. At the end nuclei were stained with Hoechst 3342 (1:1000, Cell Signaling) for 5 min at room temperature. Immunofluorescence images were acquired with Leica TCS SP5 Confocal Microscope (Leica Microsystems), z stack 0.46um, 63x of magnification and quantified measuring mean fluorescence (MFI) using ImageJ software (https://imagej.net).

3.5.2. Fluorescence dyes

NS were seeded in a 96 well plate and stained with Annexin V (556419, BD Bioscience), LysoTracker (L12492, Thermo Scientific) and Acridine Orange (6130, ImmunoChemistry Technology) for 15 min at 37°C. Images were captured using Nikon time-laps microscope (Eclipse Ti-E Nikon) at 5x and 10x magnification and MFI was measured by ImageJ software (https://imagej.net) subtracting background signal to NS emission.

3.5.3. FACS analysis

For FACS analysis NS were dissociated at single cell and filtered to avoid aggregates. For the evaluation of cell cycle, apoptosis and mitochondria ROS level, cells were washed with PBS to remove medium. For cell cycle analysis cells were fixed with ethanol 100% overnight at 4°C, washed and stained with a mix of propidium and RNAse (550825, BD Bioscience) for 15 min at 4°C. To measure early and late apoptosis cells were stained with AnnexinV (556419 BD Bioscience) for 20 min at room temperature and propidium iodide (556463 BD Bioscience) just before reading. To measure ROS levels, cells were stained with MitoSoX (1:1000 M36008, Molecular Probes) in HBSS (Gibco) for 10 min at 37°C. For the evaluation of mitochondria depolarization, cells were stained with TMRE 50nM (Invitrogen) in cell medium for 10 min at 37°C. Sample were read at FACS Canto 1 (BD Bioscience), while FACS data analysis were performed using FlowJo software (www.flowjo.com).

3.6. Clonogenicity and Invasion assays

For clonogenicity assay NS were seeded in 96 well plate (1 NS/well) and were disaggregated as single cell. Sphere formation was evaluated after 72h from seeding.

For invasion ability, 2-3 NS were seeded in collagen matrix and cells movements were monitored for 72h. The distance of single cells from sphere periphery was measured by ImageJ (https://imagej.net) and Volocity (6.3, https://www.quorumtechnologies.com/volocity). For both experiments, images were captured using Nikon time-laps microscope (Eclipse Ti-E Nikon) at 5x of magnification.

3.7. RNA extraction and gene expression evaluation

Total RNA was extracted using MasterPure RNA purification Kit (Epicentre, Illumina) and quantified by Nanodrop1000 (Thermo Scientific). 300ng of total RNA was retrotranscribed using MultiScribe™ Reverse Transcriptase (Thermo Scientific). Gene expression was evaluated by TaqMan probes (Thermo Scientific) using 10ng of cDNA and β-2-microglobulin as housekeeping gene.

3.8. Metabolism evaluation

Extracellular glucose, lactate and intracellular ATP were evaluated using commercial kits following manufacturer's instructions (respectively: BioVision K606-100, BioVision K607-100 and Enzo ALX-850-247). Glucose and lactate levels were measured by SAFAS spectrophotometer (OD 570nm), using 1µl of cell medium, while bioluminescence, proportional to ATP level, was detected by Infinite F200 (Tecan) using 10µl of cell lysate.

3.8.1. LO co-culture

Low-V1G1 NS were seeded in 24 well-plate and were co-cultured for 48 h with LO isolated from High-V1G1 NS (the equivalent of 1 ml of supernatant). After 48h Low-V1G1 supernatant and cells lysate were used for metabolic studies. LO from High-V1G1 were isolated as described in Bertolini et al., 2019 [75]. Briefly, cells supernatant was centrifuged at 1000 rcf for 10 min 4°C to eliminate cell debris and then centrifuged at 10000 rcf for 30 min at 4°C. LO pellet was washed and resuspended in PBS.

4.RESULTS

4.1. Characterization of Low and High-V1G1 neurospheres

We recently demonstrated that there is a switch in V-ATPase conformation from low grade glioma to glioblastoma with an enrichment in V1G1 subunit expression [74]. Furthermore, we showed that High-V1G1 glioma reprograms the tumour microenvironment through extracellular vesicles loaded with oncogenic cargoes [75]. In this context, we decided to further characterize neurospheres (NS) according to V1G1 expression (i.e. Low-V1G1 NS and High-V1G1 NS).

First of all, since V-ATPAse proton pump plays an important role in lysosome function [31], we analysed lysosomes acidification measured as LysoTracker intensity (Fig.7A). High-V1G1 NS showed a higher proton pump activity in comparison with Low-V1G1 NS.

Moreover, High-V1G1 NS revealed a more aggressive phenotype, meaning higher ability to invade when imbedded in 3D matrix *in vitro* (Fig.7B), to form spheres after disaggregation (Fig.7C) and to grow *in vivo* after 109 days from intracranial orthotopic injection (Fig.8 A-B). After luciferase-NS injection, tumour growth in mice was monitored every week acquiring bioluminescent signal. Before day 63 the two NS populations showed a similar trend, with a low cell growth, while after day 63, only High-V1G1 NS showed an increase of proliferation, confirmed also by the higher positivity for Ki67 staining at day 109 (Fig.8C).

From a cell biology point of view, we had previously observed by a reporter array that among the different pathways analysed, ERK was differentially modulated between High and Low-V1G1 NS. This result

was confirmed also by western blot, where High-V1G1 NS showed higher levels of phospho-ERK (Fig.7D).

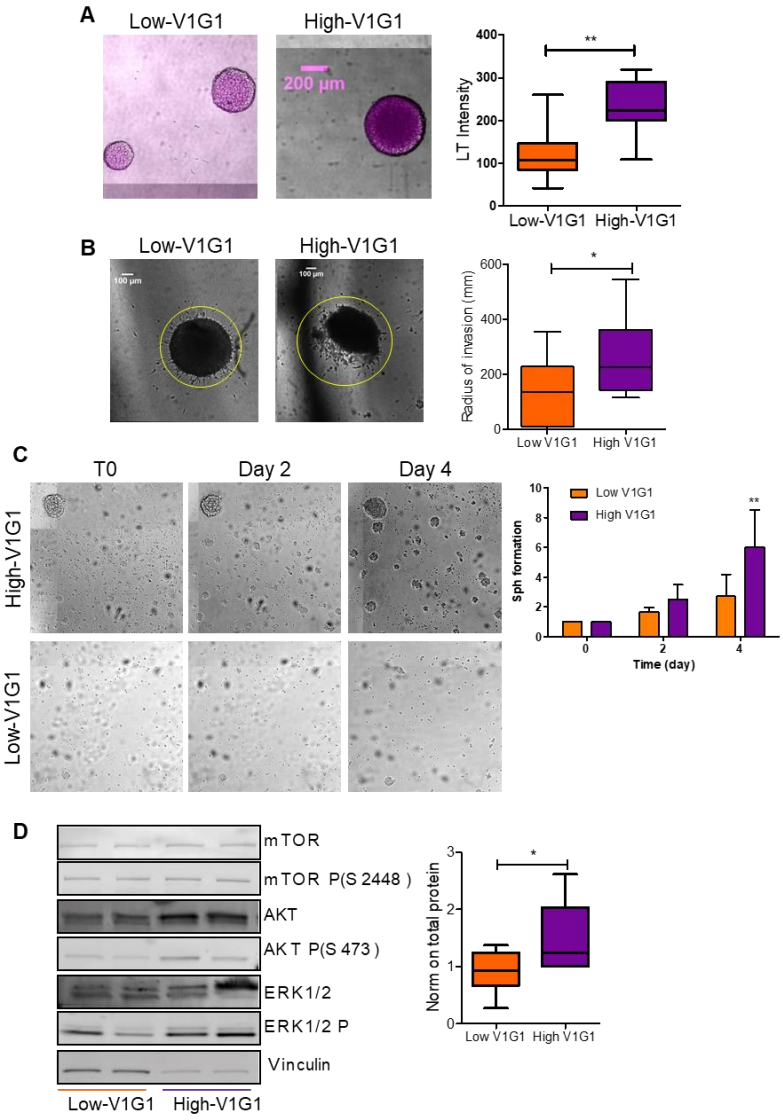

Fig.7 Low and High-V1G1 NS characterization

Lysosomal acidification (LysoTracker, A), invasion ability (B) and sphere formation (C) were measured in Low and High-V1G1 NS. Images were acquired by Nikon time laps microscope (5x of magnification) and were analysed using ImageJ and Volocity software. (D) Phospho and total proteins were measured by western blot analysis loading 40µg of cell lysates normalizing on vinculin. Statistic: Mann-Whitney t-test for LT (p=0.001), invasion (p=0.045) and pERK (p=0.047); 2way Anova Bonferroni posttests for sph formation (p<0.01).

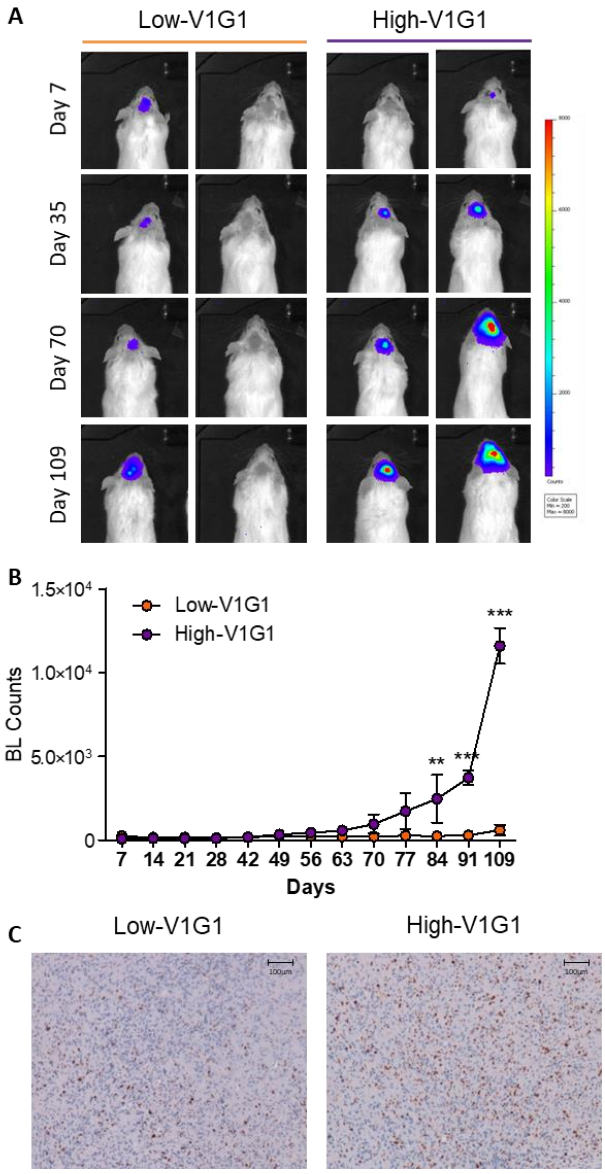

Fig 8 High-V1G1 grow *in vivo*

(A-B) In vivo cell growth was quantified measuring bioluminescence signal (BL) using the IVIS SPECTRUM/CT instrument (Perkin Elmer) for 109 days from cells intracranial injection. Statistics: Two-ways ANOVA 84 days $p<0.01$, 91 and 109 days $p<0.001$.

(C) Ki67 staining of mice brains after 109 from NS intracranial injection. Images were obtained by Leica Aperio AT2 instrument.

4.2. BafilomycinA1 effect on High and Low-V1G1 NS

The anti-V-ATPase specific drug BafilomycinA1 (BafA1) was able to decrease lysosomal acidification at non-toxic dose in both type of NS (Fig.9 A and B), but it had a greater effect in High-V1G1 NS (Fig.9B). More interestingly, BafA1 was able to decrease ERK phosphorylation only in High-V1G1 NS (Fig.9C).

Moreover, the inhibition of V-ATPase proton pump decreased invasion ability of High-V1G1 NS (Fig.9D-E), at both low and high dosage.

We have already demonstrated that BafA1 treatment induces cell death in NS at high dosage [27], but we have not studied the effect on the two populations independently. So, we investigated whether BafA1 treatment had different effects in High and Low-V1G1 NS. To do this, we analysed BafA1 effect on the percentage of AnnexinV-positive cells. In figure 10, images (A and B) and graphs (C and D) confirm that the drug can induce cell death at high dosage, but only in High-V1G1 NS (Fig.10B-D), indicated by the high level of AnnexinV fluorescence signal after BafA1 treatment.

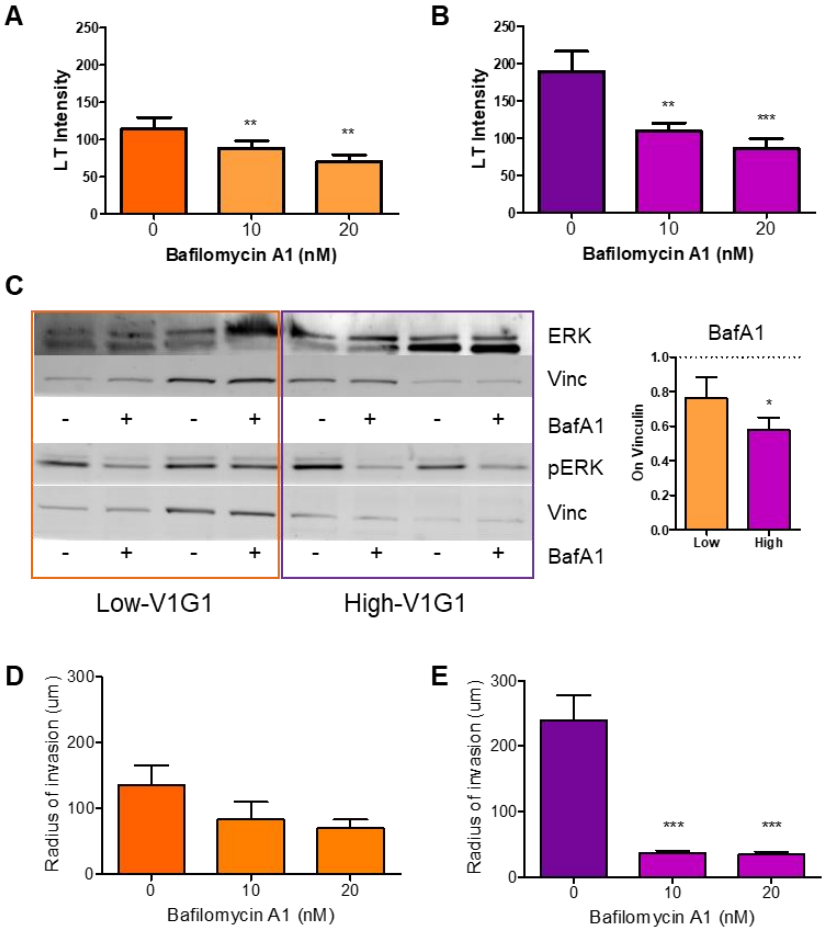

Fig.9 BafA1 effect on lysosomes and ERK phosphorylation

(A-B) Lysosomal acidification (LysoTracker) was measured in Low (A) and High-V1G1 (B) NS after 24h of 10 and 20nM BafA1 treatment. (C) Phospho ERK level was measured by western blot at basal condition and after 24h of BafA1 treatment (10nM). 40µg of cell lysates were loaded, pERK level was normalized on vinculin and on total protein. ERK phosphorylation level after BafA1 treatment was compared to CTRL samples.

(D-E) Invasion ability was measured in Low and High-V1G1 NS after 24h of 10 and 20nM BafA1 treatment

Statistic: Wilcoxon matched-pairs t-test. A: BafA1 10nM p=0.079, BafA1 p=0.001; B: BafA1 10nM p=0.005, BafA1 p=0.0005. C: p=0.043. D-E 1 Way Anova Dunn's Multiple Comparison test p<0.0001.

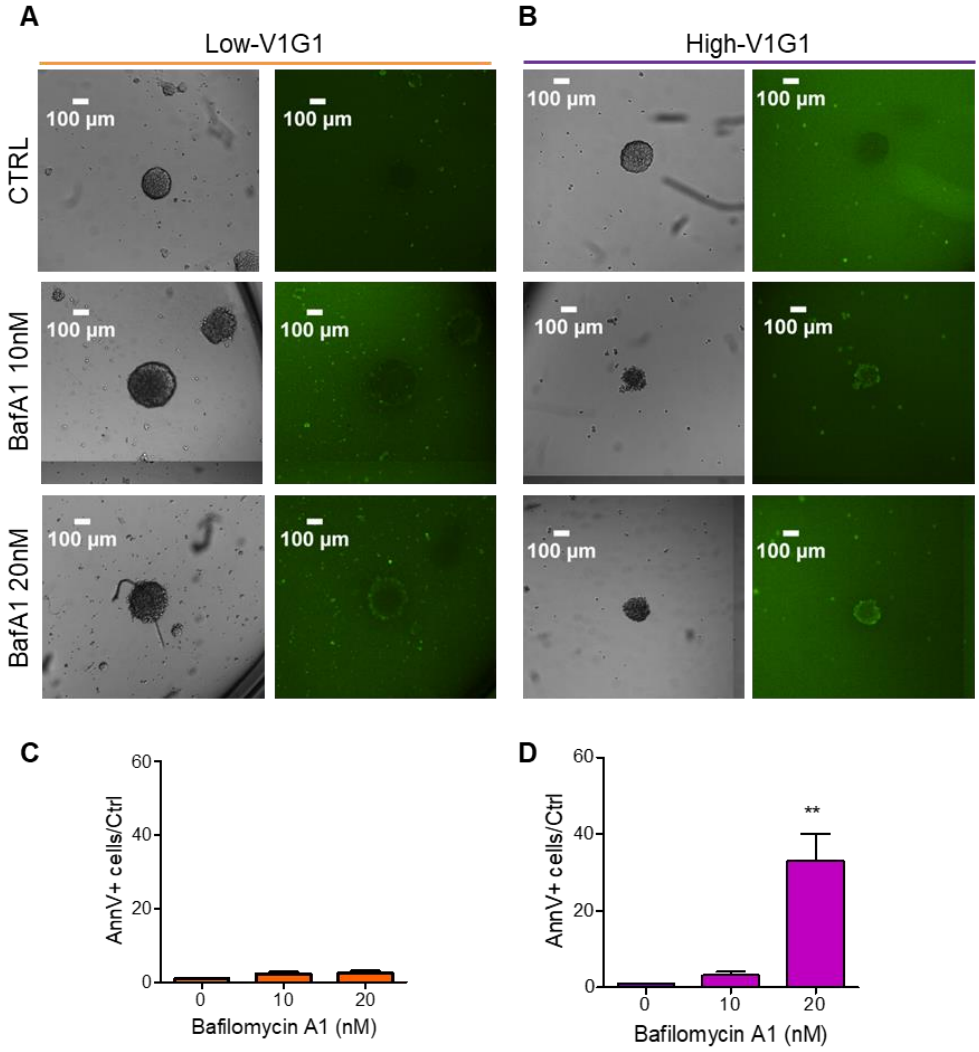

Fig. 10 BafA1 induces cell death only in High-V1G1 NS

(A-B) Images of NS were obtained using Nikon time laps microscope and were analyzed using ImageJ software, subtracting background and normalizing fluorescent signals on total spheres area.

(C-D) AnnexinV signal was evaluated after 24h of BafA1 treatment at 10nM and 20nM in Low (A-C) and High-V1G1 (B-D) NS. Treatment samples results were normalized on CTRL sample. Statistic: 1way Anova – Bonferroni's multiple comparison test p=0.003

4.3. Targeting of lysosomes and MAPK/ERK pathway

Because of the different effects of BafA1 treatment in the two cell populations, with the High-V1G1 NS being the most sensitive culture, (Fig.9 and 10), we aimed to understand if these effects were specifically related to the inhibition of the V-ATPase proton pump or were due to lysosomes or ERK pathway impairment.

To this end, we compared the two cell populations after lysosomes or ERK pathway impairment using Ammonium Chloride (NH_4Cl), that causes an alteration of lysosomes acidic pH [77], or PD98059 (PD) as ERK/MEK inhibitor [78]

First, we tested the effect of the two drugs on their targets in our cellular models: acidification (Fig.11A-D) and ERK phosphorylation (Fig.11E) levels, respectively.

As expected NH_4Cl caused a decrease of cell acidification (AO) in both High and Low-V1G1 NS (Fig.11C, D), while PD had no effect (Fig.11A-D). On the other hand, PD was able to decrease ERK activation, while NH_4Cl didn't influence the phosphorylated status of ERK (Fig.11E)

As previously reported BafA1 decreased lysosomal acidification (LT, AO) in both cell populations (Fig.11A-D) and reduced ERK phosphorylation level (Fig.11E).

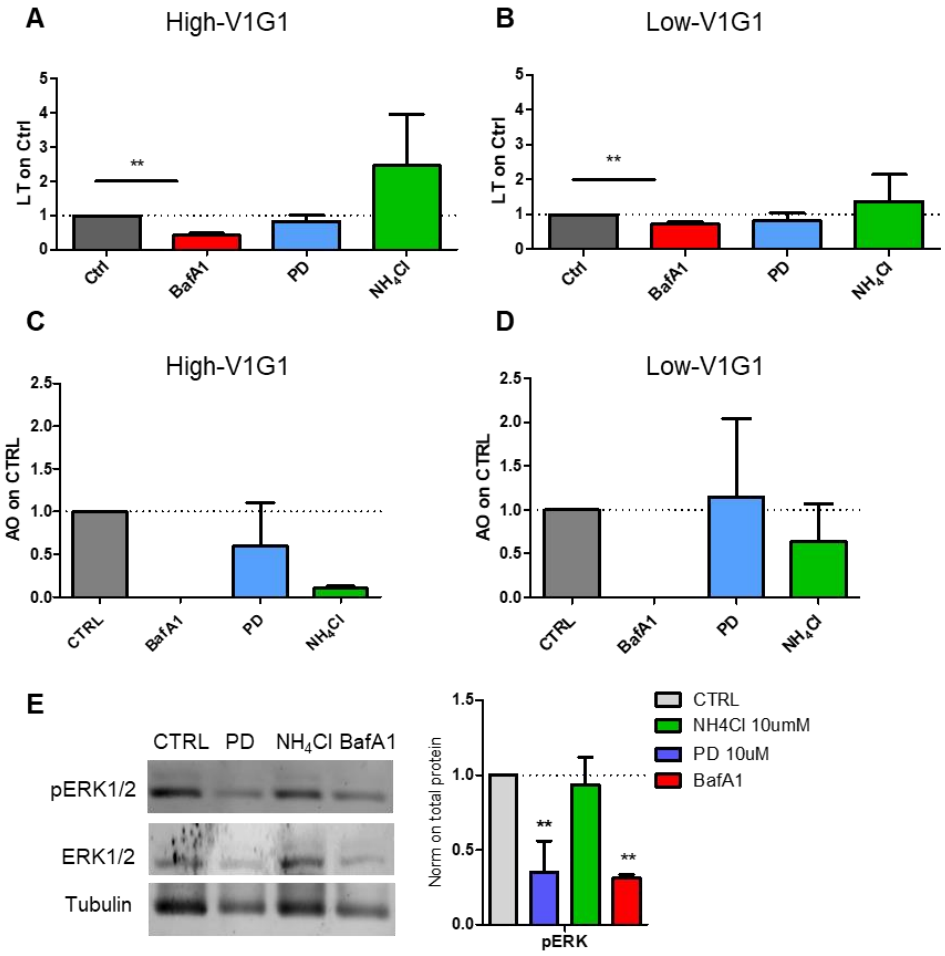

Fig.11 Effects on acidification and ERK phosphorylation after drugs treatment

(A-D) LysoTracker (A,B) and Acridine Orange (C,D) intensities were evaluated in High and Low-V1G1 NS after 24h of BafA1 10nM, PD 10µM and NH_4Cl 10mM treatments. Images were capture by Nikon time laps microscope and were analysed using ImageJ software, measuring the mean fluorescence intensity (MFI) of NS.

(E) ERK phosphorylation was evaluated by western blot analysis at basal condition and after drugs treatment in High-V1G1 NS. Quantification was performed using ImageJ software. Statistic: Mann-Whitney t-test. A p=0.004; B p=0.005; E: BafA1 p=0.003, PD p=0.007

4.4. Autophagy

Autophagy is one of the most important pathways connected with lysosomal function [79], so we compared the effect on this process after acidification impairment caused by BafA1 and NH_4Cl treatment.

As marker of autophagic flux we used p62, that is involved in the last steps of the process. If the autophagic flux is blocked, p62 should accumulate and therefore its expression levels increased [80].

We started analysing the levels of this protein after 24h of drugs treatment. Immunofluorescence results showed an increase of p62 level only after BafA1 treatment in Low-V1G1 NS, while it did not increase in High-V1G1 NS or after PD and NH_4Cl treatments (Fig.12).

This might indicate that BafA1 caused an impairment of autophagy only in Low-V1G1 NS. To verify this result we analysed p62 levels at different times to see if drugs treatment caused an accumulation of the protein (Fig.13). p62 showed a mild accumulation in Low-V1G1 NS after 9 and 12h from BafA1 treatment (Fig.13A), while the protein remained at low levels in High-V1G1 NS (Fig.13B). To confirm immunofluorescence results, we performed a time-course analysis of p62 level also after NH_4Cl treatment and it confirmed the absence of accumulation in both cellular models (Fig.13C and D).

Autophagy is characterized by the presence of autophagosomes and the block of the flux causes the impairment of their turnover [81]. To confirm the results obtained after BafA1 treatment, we analysed cells appearance by electron microscopy. Images in figure 14 evidence an increased number of autophagosomes (circled in red) in Low-V1G1

after drug treatment (left panel), while we cannot observe their presence in High-V1G1 NS (right panel).

Taken together, the accumulation of p62 and presence of autophagosomes indicated that the specific inhibition of V-ATPase blocked autophagic flux only in Low-V1G1 NS. These results suggested that in Low-V1G1 NS the block of the autophagic flux could be related to lysosomal V-ATPase, in fact we didn't observe the same effect blocking general acidification (NH_4Cl treatment). Moreover, we can speculate that in High-V1G1 cells V-ATPase pump is implicated in signalling unrelated to autophagy.

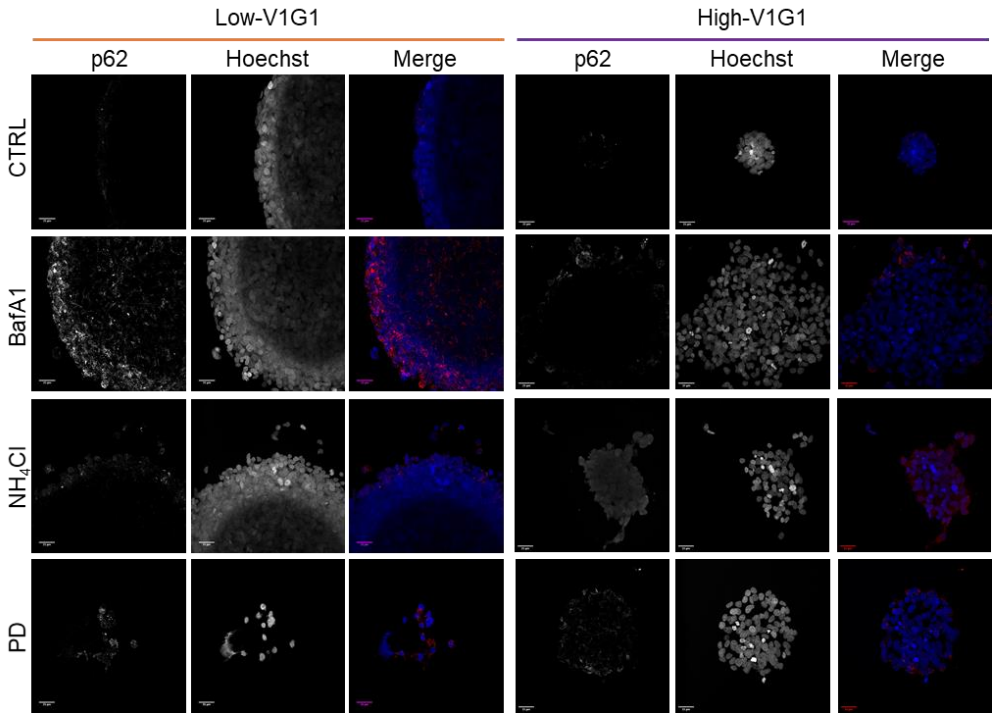

Fig. 12 Drugs effect on autophagy

p62 levels were analysed by immunofluorescence on Low (left panel) and High-V1G1 (right panel) in CTRL cells and after 24h of BafA1 10nM, PD 10µM and NH_4Cl 10mM treatments (from top to bottom).

Images were captured using Leica SP5 Confocal Microscope (magnification: 63x).

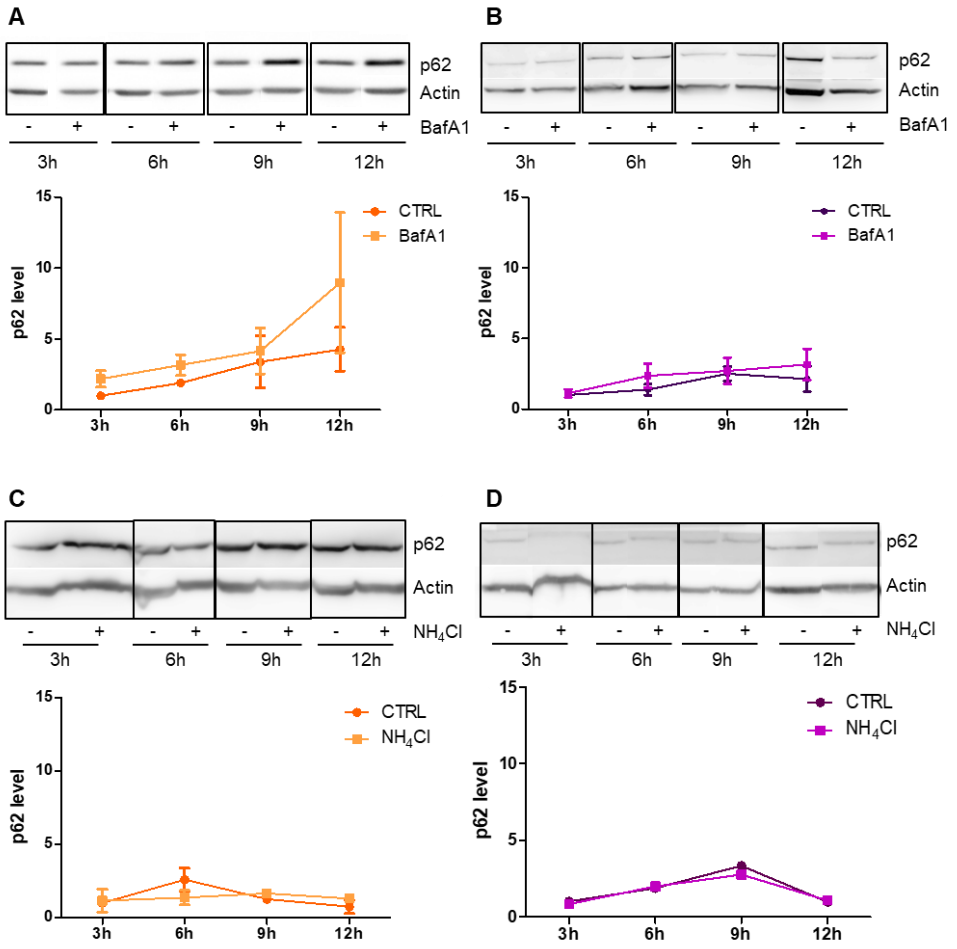

Fig.13 BafA1 impairs autophagic flux in Low-V1G1 NS

p62 level was evaluated by western blot in Low (A, C) and High-V1G1 (B, D) NS, after 3, 6, 9 and 12h of BafA1 (A, B) or NH_4Cl (C, D) treatment. 40ug of proteins from total cell lysate were loaded and β-actin was used as normalizer. Images were quantified using ImageJ software.

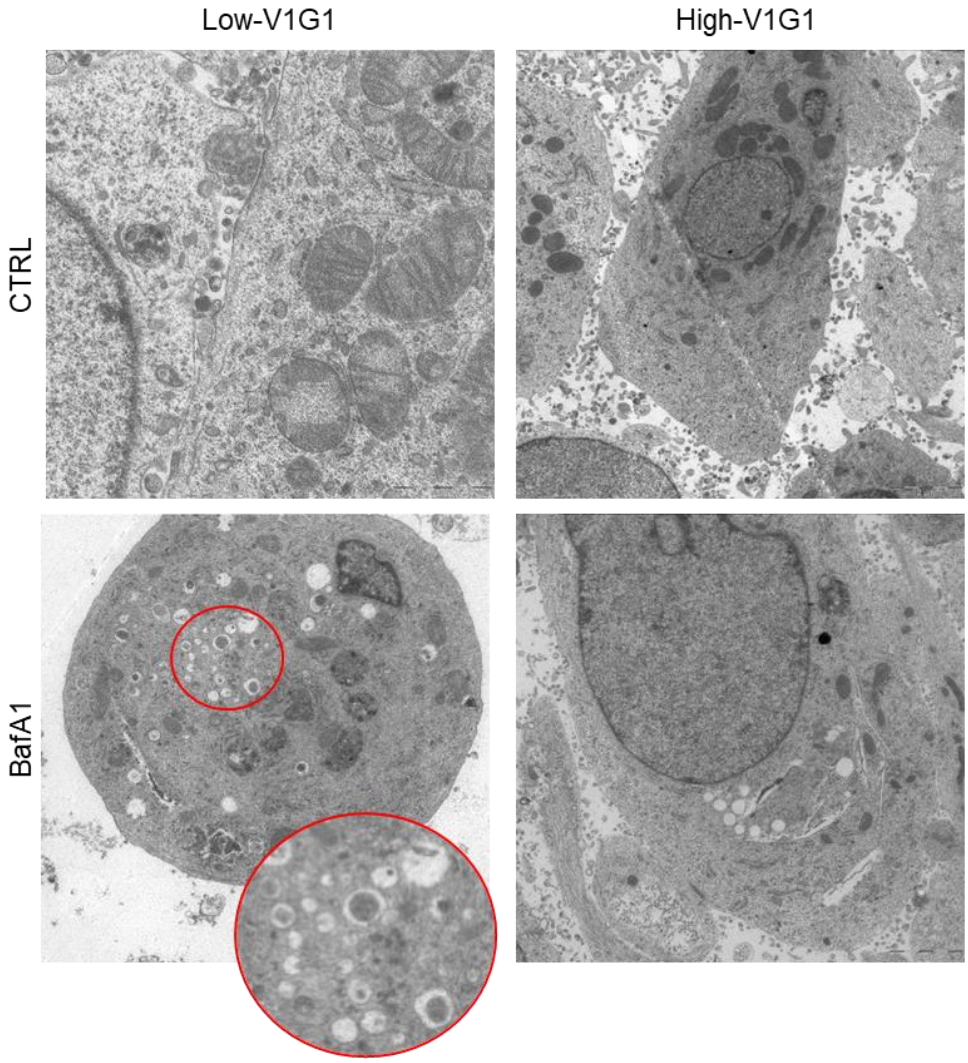

Fig. 14 BafA1 increase the number of autophagosomes in Low-V1G1
Representative images of electron microscopy of Low and High-V1G1 NS at basal condition (upper panels) and after 24h of BafA1 treatment (lower panels). Autophagosomes presence (circled in red) was evaluated using FEI Tecnai G2 20 Transmission Electron Microscope (1840X magnification).

4.5. MAPK/ERK pathway impairment

Given that BafA1 treatment modulated ERK phosphorylation in High-V1G1 NS (Fig.3C and 11E) but it was not able to impair the autophagic flux (Fig.12-13-14), we decided to further analyse ERK pathway in this cellular model using a phospho-array that allowed measuring the expression levels of MAPK phospho-proteins after BafA1, PD and NH_4Cl treatments. After treating NS with the three drugs we observed that PD and BafA1 decreased ERK1/2 and P70S6K phosphorylation, BafA1 and NH_4Cl decreased the phosphorylation of AKT 1, 2, 3 and JNK1 (Fig.15A and B), but only BafA1 decreased CREB, GSK3a/b, MKK3, MKK6 and JNK2 indicating a specific effect related to V-ATPase inhibition (Fig.15C). All of these proteins play a role in cell proliferation, cell cycle, cell motility and, especially the ones modulated by BafA1, are involved in apoptosis [82–86], so we decided to investigate these processes comparing the different pharmacological treatments.

We observed that clonogenicity was reduced mostly by BafA1 treatment (Fig.16A). Conversely, cell invasion was reduced by both BafA1 and PD (Fig.16B).

Finally, cell cycle progression was impaired only after BafA1 (Fig.17A) with a block in G2/M phase (Fig. 17B) [87].

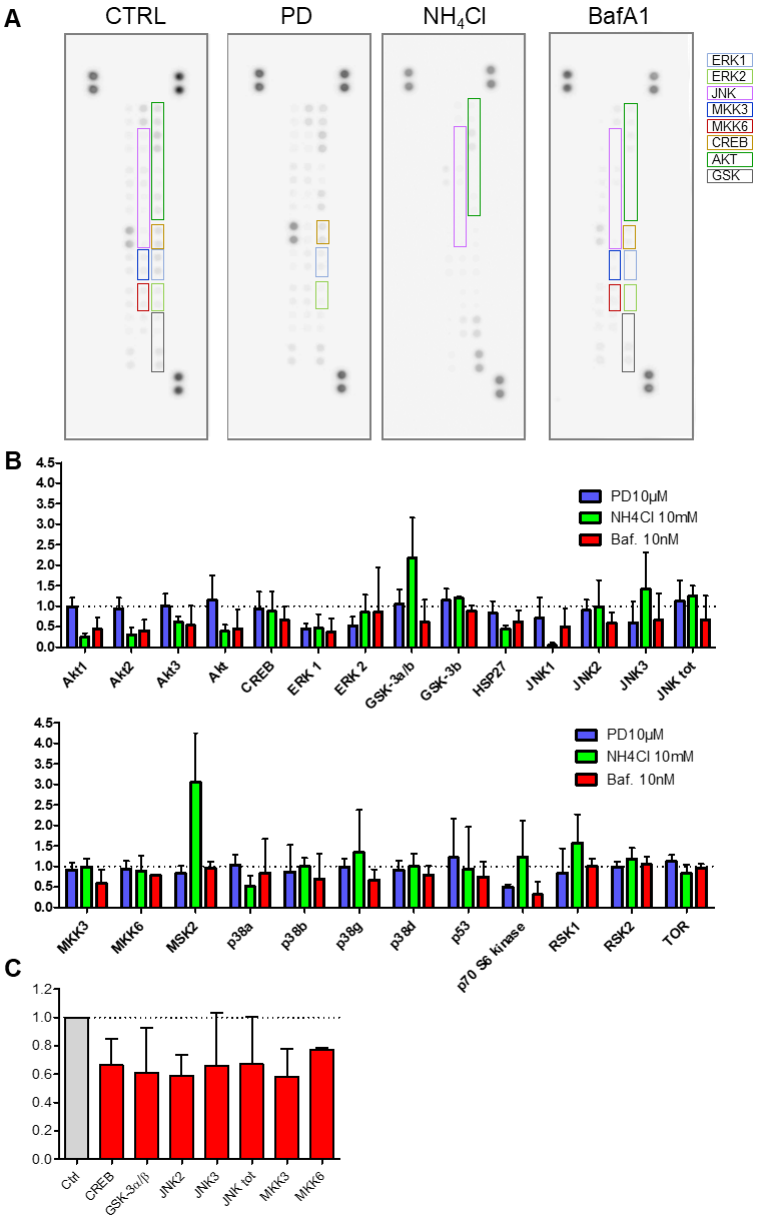

Fig. 15 Drugs effects on MAPK/ERK pathway

(A) Modulation of phospho-protein of MAPK/ERK pathway was evaluated in High-V1G1 NS using a phospho-MAPK-array after 24h of PD 10µM, NH_4Cl 10mM and BafA1 10nM treatment. (B-C) Phosphorylation levels of the total array (B) and of BafA1 modulated proteins (A). Spots intensity were evaluated by ImageJ software and were normalized on CTRL signals.

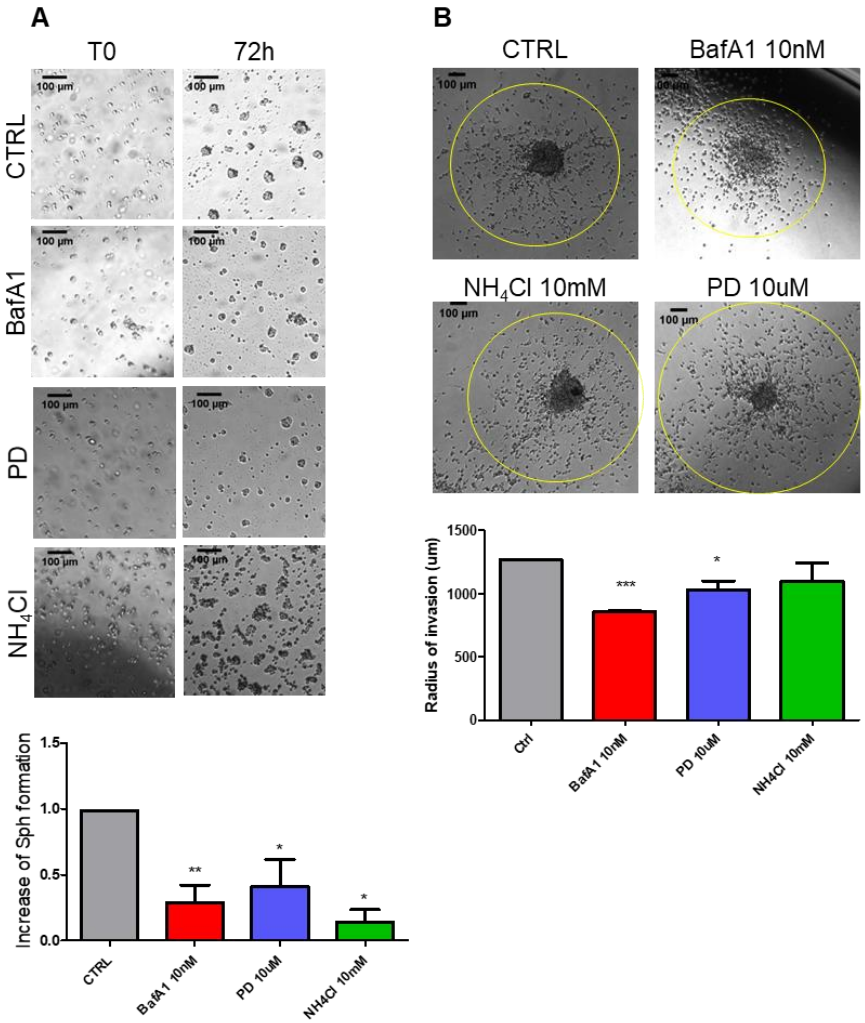

Fig.16 Drugs effects on clonogenicity and invasion

(A) Clonogenicity was evaluated as number of NS formed after the dissociation of a single sphere after 72 h. (B) Invasion was evaluated as migration in collagen (circled in yellow) after 48 h from seeding. The two experiments were performed on High-V1G1 NS treated with BafA1, PD and NH_4Cl at the indicated concentrations. Images were captured by Nikon time laps microscope (5x of magnification) and were analyzed using ImageJ software. Statistic: Mann-Whitney t-test A: BafA1 p=0.005, PD and NH4Cl p=0.01; B: BafA1 p<0.0001, PD p=0.038.

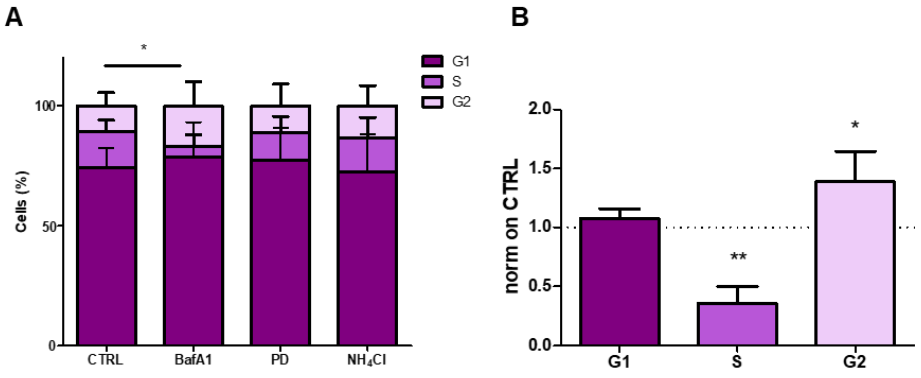

Fig. 17 Drugs effects on cell cycle

(A) Cell cycle modulation was evaluated after 24h of drug treatments (BafA1 10nM, PD 10µM and NH_4Cl 10mM) by flow cytometry.

(B) G1, S and G2 phases after BafA1 treatment normalized on CTRL level. Data were analyzed using FlowJo software. Statistic: Mann-Whitney t-test. A BafA1 p=0.01; B S phase p=0.009, G2 p=0.015.

4.6. Cell death mechanism in High and Low V1G1 NS

4.6.1. Apoptosis induction in High VG1 NS

To study if the induction of cell death was specifically caused by V-ATPase inhibition or to ERK or lysosomes impairment, we compared BafA1 effects to the other two drugs in High-V1G1 NS.

Only BafA1 treatment caused a slight increase of both AnnexinV and AnnexinV/PI positive cells, compared to CTRL sample, indicating the presence of cells in early and late apoptosis respectively (Fig.18A). On the other hand, PD and NH_4Cl treatments showed a moderate increase of the AnnexinV/PI-positive fraction (Fig.18A).

In all the four conditions, however, there was high level of PI positive cells that indicate necrosis, probably due to the hypoxic and necrotic core of spheroids [88,89].

The activation of apoptosis after BafA1 treatment was also confirmed by an imbalance in the ratio between the anti-apoptotic (BCL2) and pro-apoptotic (BAK, BAX and BIK) BCL-family genes (Fig.18B)

To confirm the previous experiments (Fig.10) we analysed the presence of AnnexinV/PI positive cells in Low-V1G1 NS after BafA1 treatment and, as expected, there was no activation of apoptosis (Fig.19), but only high level of necrosis.

These data indicated that V-ATPase activity was essential for GBM stem cell viability and, again, this suggests that it could be implicated in other processes other than ERK pathway and lysosomal acidification.

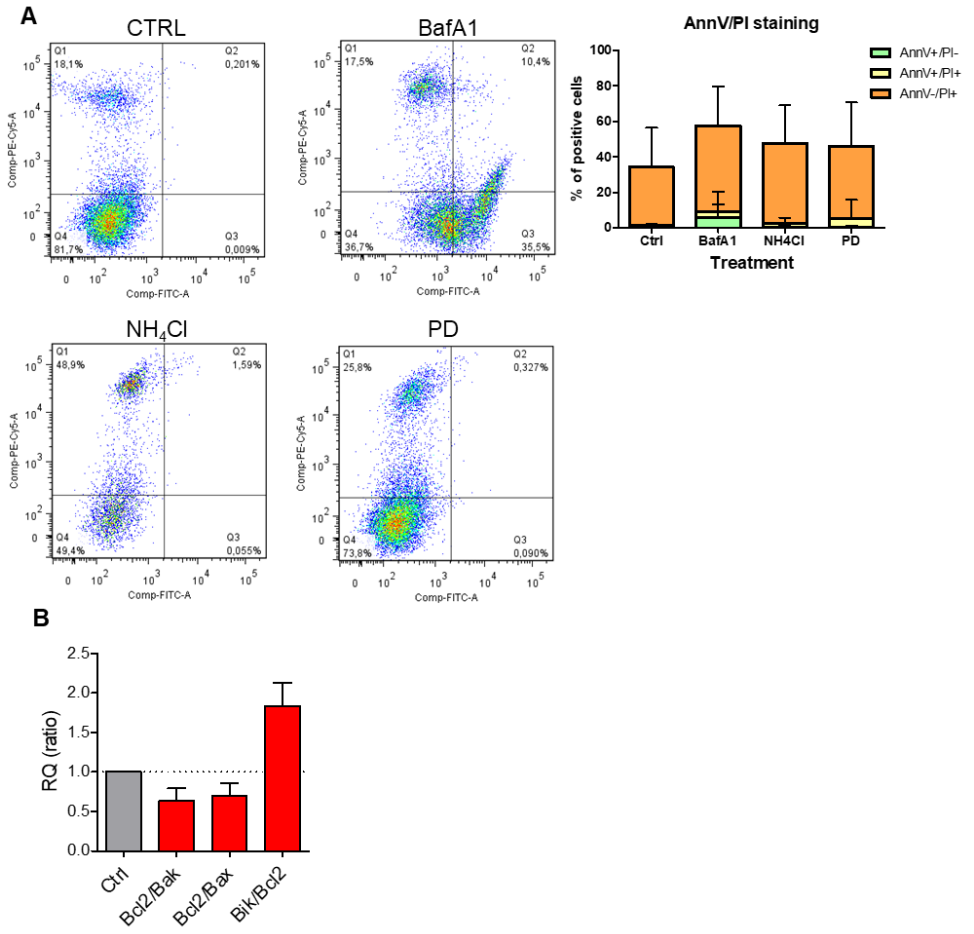

Fig. 18 BafA1 induced apoptosis in High-V1G1 NS

(A) Apoptosis induction was evaluated by flow cytometry using FACS Canto 1 (BD Bioscience) as increase of AnnexinV and AnnexinV/PI positive cells. High-V1G1 NS were treated for 24h with BafA1 20nM, PD 10µM and NH_4Cl 10mM. FACS data were analyzed by FlowJo software.

(B) Pro and anti-apoptotic genes expression was evaluated by qPCR using β2-microglobulin as housekeeping gene.

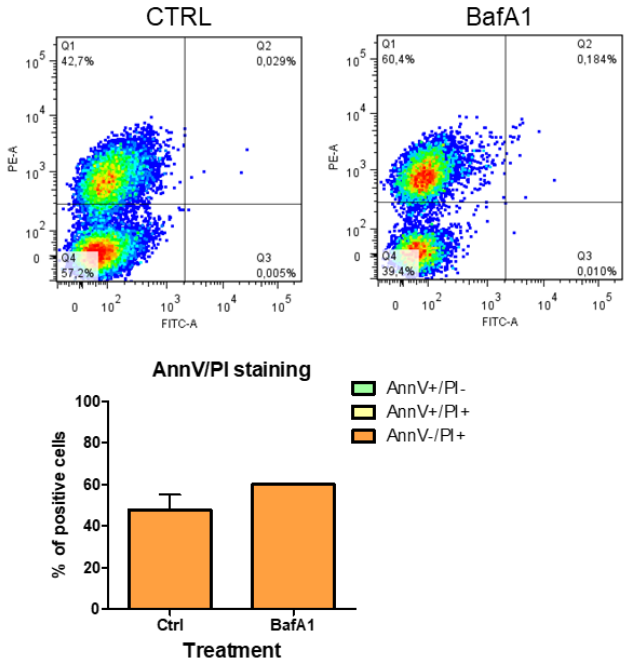

Fig. 19 Apoptosis in Low-V1G1 NS after BafA1 treatment

Apoptosis was evaluated in Low- V1G1 NS after BafA1 20nM treatment. AnnexinV and PI positive cells were measured by flow cytometry using FACS Canto 1 (BD Bioscience). Data were analysed by FlowJo software.

4.6.2. The role of ROS production in the induction of cell death

Apoptosis is directly connected with mitochondrial ROS production, so we analysed their level in the two cellular models after BafA1, NH_4Cl or PD treatments (Fig.20).

BafA1 was the only drug able to increase mitochondria ROS production in High-V1G1 NS (Fig.20A). As expected BafA1 treatment did not increase ROS level in Low-V1G1 NS (Fig.20B).

To confirm the relation of ROS production and apoptosis induction, we treated High-V1G1 NS with the combination of BafA1 and an inhibitor of ROS that, after 24h, restored ROS levels to baseline. Furthermore, ROS inhibition decreased the percentage of apoptotic cells in BafA1-treated samples (Fig.21A and B).

As control we performed the same experiment in Low-V1G1 NS, but as expected, there was no effect (Fig.21C and D).

These results indicated that the specific inhibition of V-ATPase proton pump in High-V1G1 NS increased mitochondrial ROS that was directly connected to the activation of apoptosis.

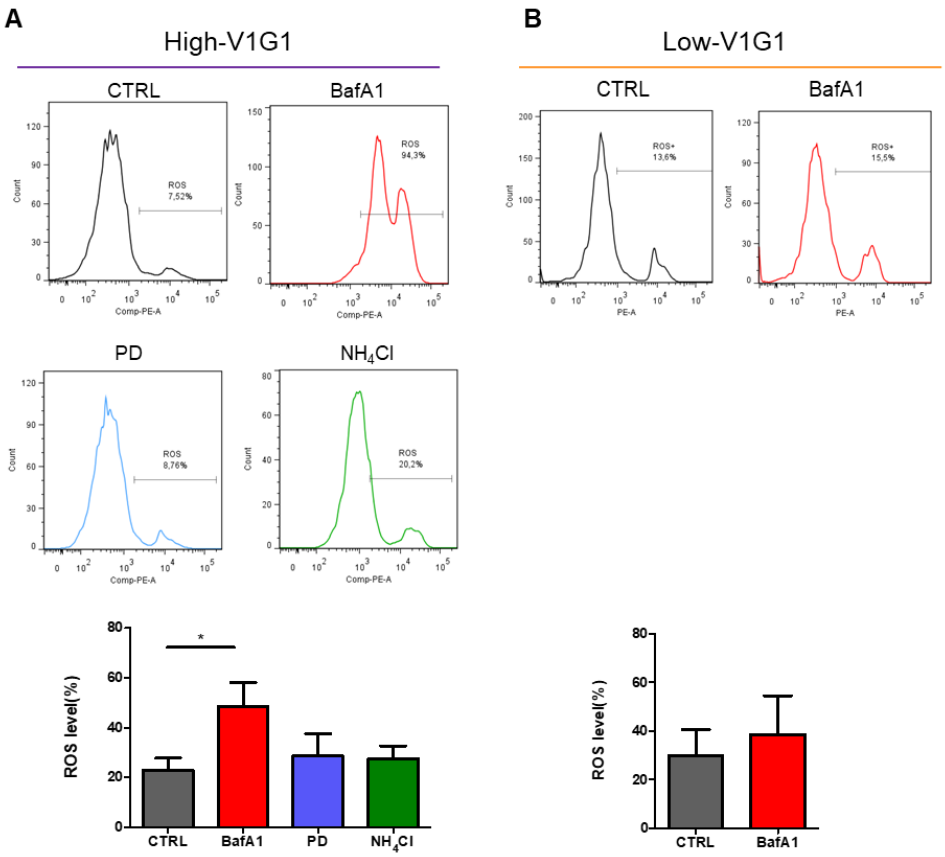

Fig. 20 BafA1 treatment increases ROS level in High-V1G1

(A, B) Mitochondria ROS level was measured by staining with MitoSox reagent in High-V1G1 NS after 24h of BafA1 20nM, PD 10μM and NH_4Cl 10mM treatment (A) and in Low-V1G1 NS after 24h of BafA1 20nM treatment (B). Data were analyzed by FlowJo software. Statistic: Mann-Whitney t-test. A p=0.031

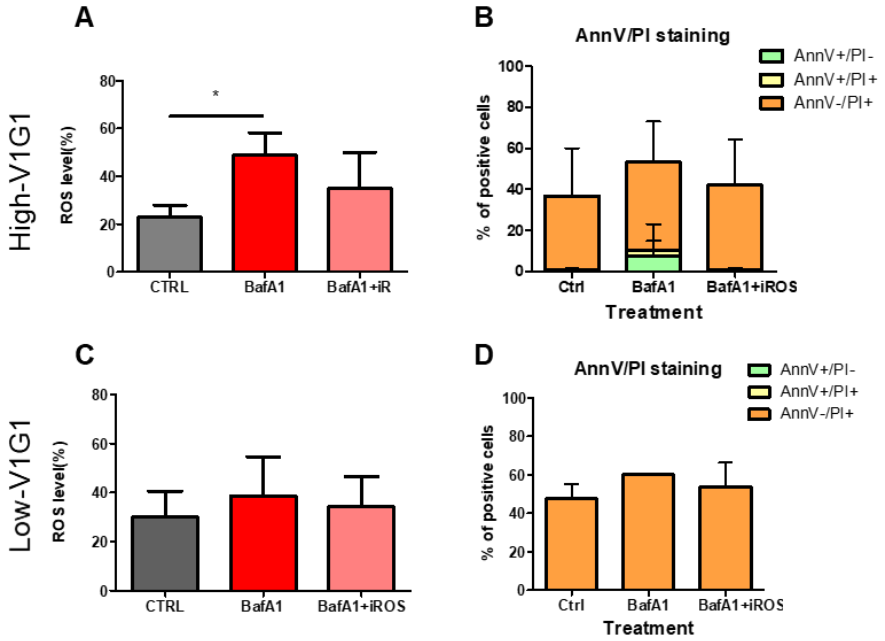

Fig. 21 The inhibition of ROS production reverts BafA1 effects in High-V1G1 NS

ROS Level (A, C) and apoptosis (B, D) were evaluated by flow cytometry (FACS Canto 1, BD Bioscience). High-V1G1 (A, B) and Low-V1G1 (C, D) NS were treated for 24h with BafA1 20nM and a combination of BafA1 and ROS inhibitor. Data were analyzed by FlowJo software. Statistic: Mann-Whitney t-test. A p=0.031

4.7. Mitochondria activity

Because we showed that BafA1 induced ROS-dependent apoptosis in High-V1G1 NS, we investigated whether V-ATPase activity could alter mitochondria homeostasis in High-V1G1 NS. To this purpose, after BafA1 treatment High and Low-V1G1 NS were stained with TMRE, a cationic fluorescent dye internalized in mitochondria when the matrix is more negative, allowing to study the activity and polarization level of this organelle. After V-ATPase inhibition for 48h with BafA1 at not lethal dosage (10nM) High-V1G1 NS showed a lower value of TMRE positive cells in comparison with CTRL sample (Fig. 22A), indicating a decrease of mitochondria activity or an increase of their depolarization or damage.

In Low-V1G1 NS, instead, BafA1 treatment did not affect mitochondria polarization/activity.

To further analyse mitochondrial activity, we compared the levels of mitochondria enzymes after BafA1 treatment. Therefore, we purified mitochondria extracts in NS after BafA1 or vehicle incubation.

Our data showed that there was a general reduction of mitochondrial enzymes levels in High-V1G1 NS and a reduction of VDAC located on the outer membrane of mitochondria after V-ATPase block compared to control (Fig. 22B).

These results indicated that the inhibition of V-ATPase had an effect also on mitochondria activity that might suggest a physical connection with the proton pump and this organelle.

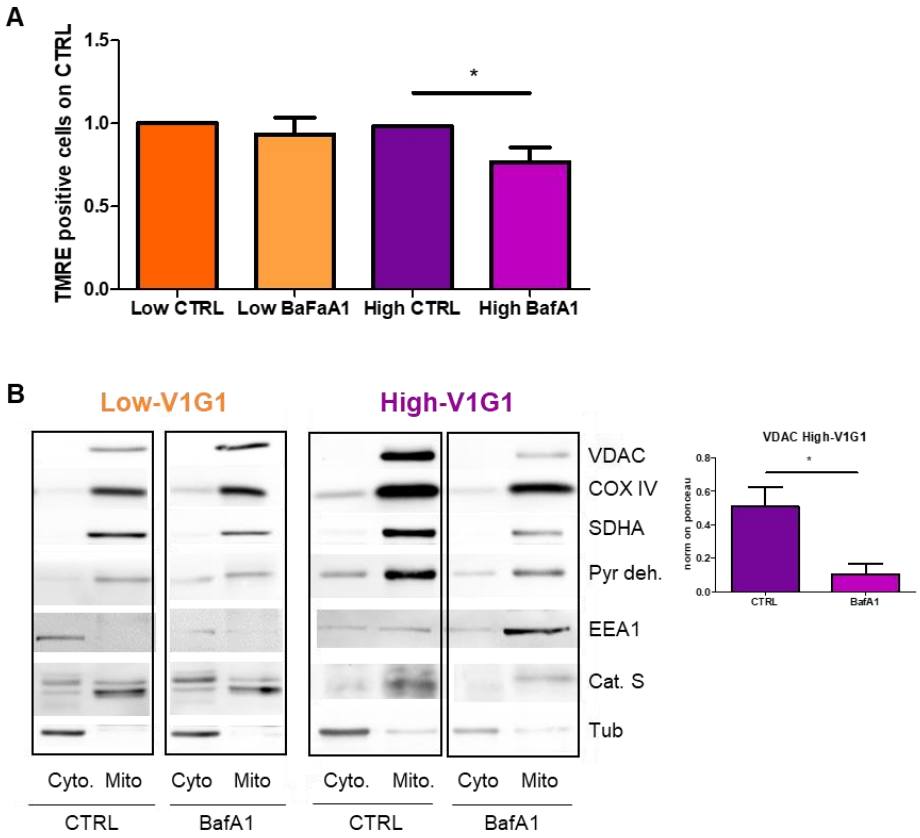

Fig. 22 BafA1 affects mitochondria activity/polarization in High-V1G1 NS

(A) Mitochondria activity/polarization was evaluated by flow cytometry, staining NS with TMRE after 24h of BafA1 10nM treatment. (B) Mitochondrial enzymes were evaluated by western blot, loading 15µg of cytoplasmic and mitochondria protein extracts. EEA1, cathepsin S and tubulin were used as markers of mitochondrial fraction purity. NS were treated with BafA1 10nM for 24h. Mitochondrial proteins level were measured by ImageJ software and signals were normalized on ponceau. Statistic: Mann-Whitney t-test. A p=0.01; B p=0.038.

4.8. Metabolic behaviour of High and Low-V1G1 NS

We were also interested in understanding if different V-ATPase conformations were also related to NS metabolic activities besides being indicative of different tumorigenic behaviours [74]. Moreover, the effect of V-ATPase inhibition on mitochondria homeostasis suggested that different V-ATPase activity or conformation could alter cell bioenergetics. Therefore, we characterized the two cellular models from a metabolic point of view, at basal condition and after V-ATPase signalling perturbation.

4.8.1. Characterization of basal metabolism

Metabolic characteristics of Low and High-V1G1 NS at basal condition were studied evaluating extracellular lactate (Fig.23A), glucose (Fig.23B) and intracellular ATP (Fig.23C). Low-V1G1 NS showed higher levels of extracellular lactate and ATP, while glucose level was higher in High-V1G1 NS. These results indicate a different bioenergetics requirement of the two cells population. Further, this evidence was confirmed by the expression levels of the two LDH isoforms, the enzymes responsible of the interconversion between lactate and pyruvate [90]. According to lactate measurements, LDHA, that promotes the production of lactate from pyruvate, was higher in Low-V1G1 NS (Fig.23D), while LDHB, that catalyses the conversion of lactate in pyruvate, was increased in High-V1G1 NS (Fig.23E). The two transporters responsible of lactate export (MCT1, Fig.23F) and glucose uptake (Glut1, Fig.23G) were also evaluated by immunoblotting but they did not show differences in the two cell populations.

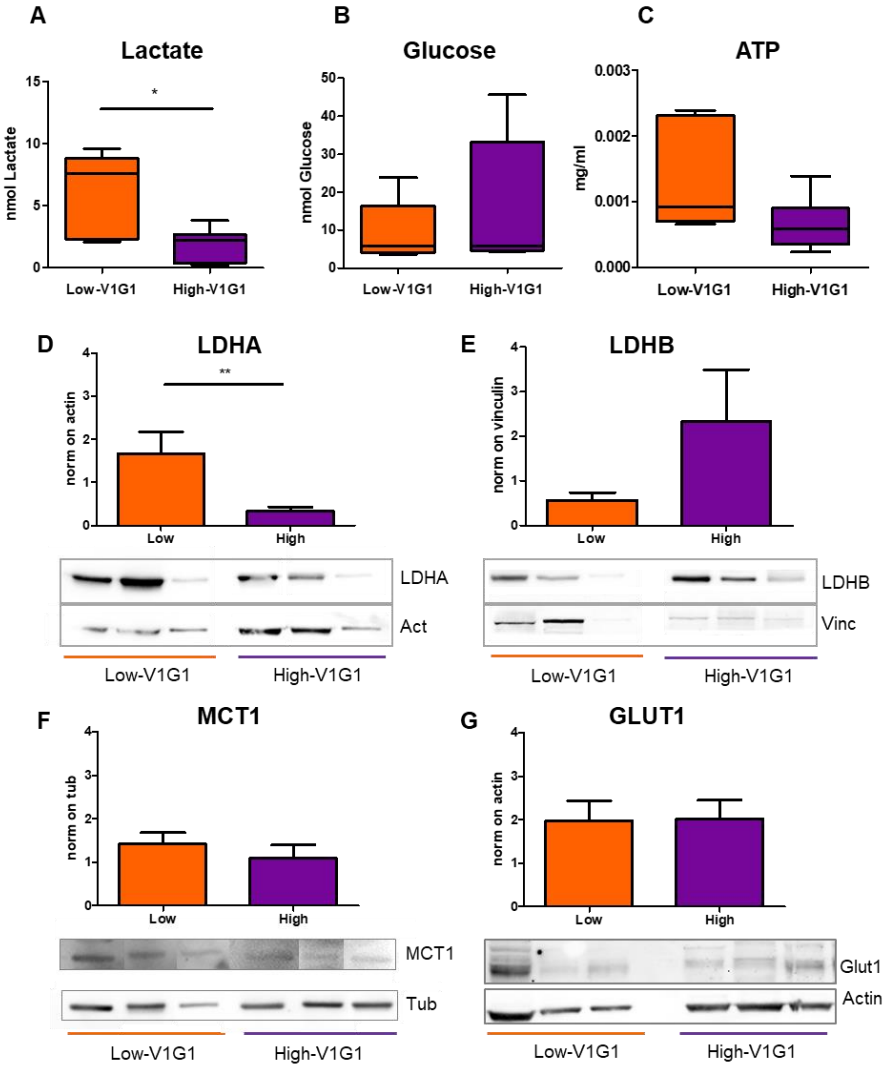

Fig.23 Metabolic behaviour of High and Low V1G1 NS at basal condition

(A) Extracellular lactate, (B) glucose and (C) intracellular ATP were evaluated at basal condition using supernatant or cell lysate. (D-G) Metabolic enzymes (LDHA; LDHB; MCT1 and GLUT1) were evaluated by western blot, loading 40µg of proteins from total cell lysate. β-actin, β-tubulin and vinculin were used as normalizers. Statistic: Mann-Whitney t-test. A p=0.018; D p=0.001

4.8.2. Change in metabolic behaviour after BafA1 treatment

Given that High and Low-V1G1 NS seemed to have different metabolic behaviour at basal condition, we investigated if inhibition of V-ATPase activity in High-V1G1 was able to recoup bioenergetics to Low-V1G1 condition.

BafA1 treatment induced a slight increase of lactate production and LDHA levels in High-V1G1 NS, while it had no effect in Low-V1G1 (Fig. 24A and D). Levels of extracellular glucose (Fig. 24B), intracellular ATP (Fig. 24C), LDHB (Fig. 24E) and the two transporters, GLUT1 (Fig. 24F) and MCT1 (Fig. 24G), were not affected by pharmacological treatment.

These results indicated that the impairment of V-ATPase induced a shift of metabolism that became more similar to Low-V1G1 NS metabolic behaviour.

4.8.3. Reprogramming metabolic behaviour after Large Oncosomes co-culture

Large Oncosomes (LO) are a class of extracellular vesicles able to modify microenvironment [75,76].

In our laboratory it was previously demonstrated that LO isolated from High-V1G1 NS supernatant vehiculate V1G1 subunit and are able to reprogram recipient cells in terms of tumorigenicity and aggressiveness [75]. Because of these observations we investigated if they also brought signals able to modify the metabolic behaviour of Low-V1G1 NS.

The co-culture decreased lactate production ability of Low-V1G1 NS (Fig. 25A) after 48h, while there was no modulation of the enzymes involved, except for a slight decrease of Glut1 (Fig.25B).

Taken together, these results suggested that V-ATPase proton pump activity is involved in the regulation of metabolic behaviour of glioma stem cells.

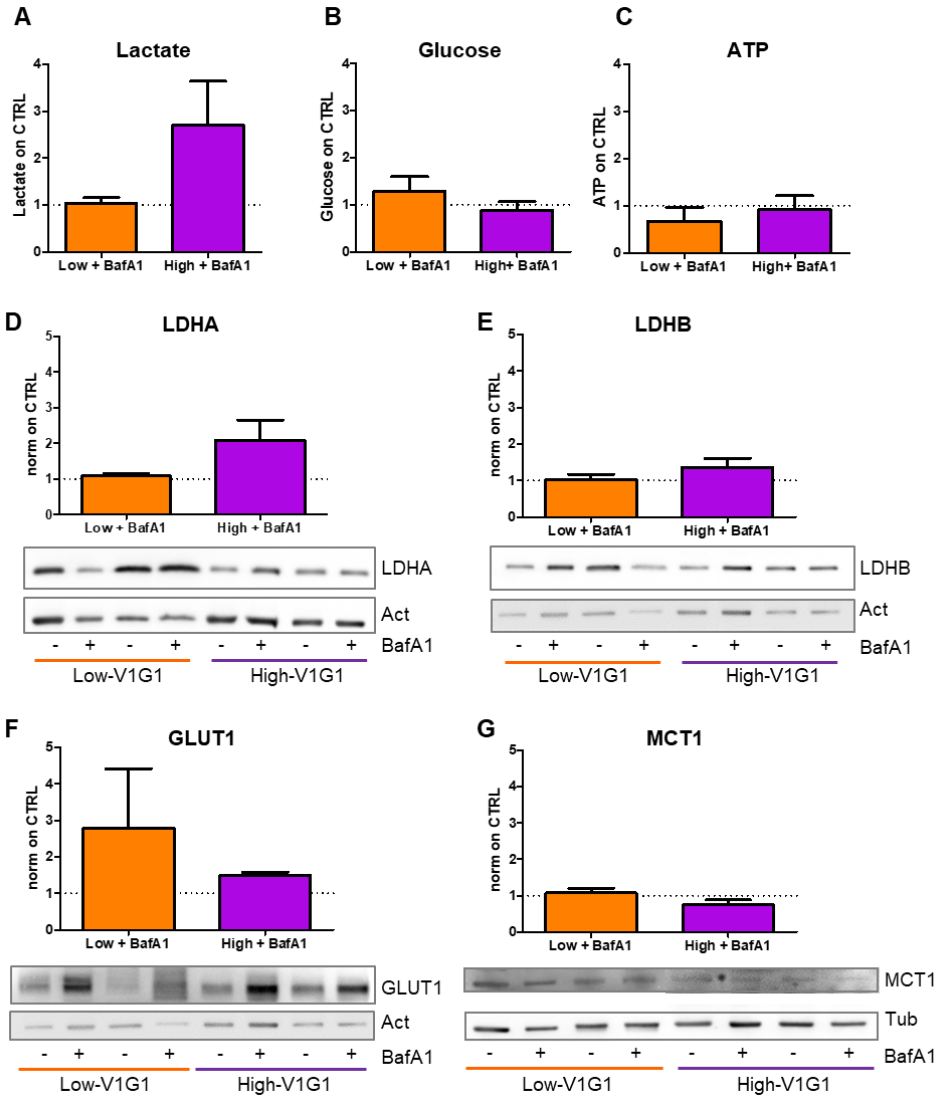

Fig.24 BafA1 treatment modifies metabolic behaviour of High-V1G1 NS

(A) Extracellular lactate, (B) glucose and (C) intracellular ATP were evaluated after 24h of BafA1 10nM treatment using supernatant or cell lysate. (D-G) Metabolic enzymes (LDHA; LDHB; MCT1 and GLUT1) were evaluated by western blot, loading 40µg of proteins from total cell lysate. β-actin and β-tubulin were used as normalizers.

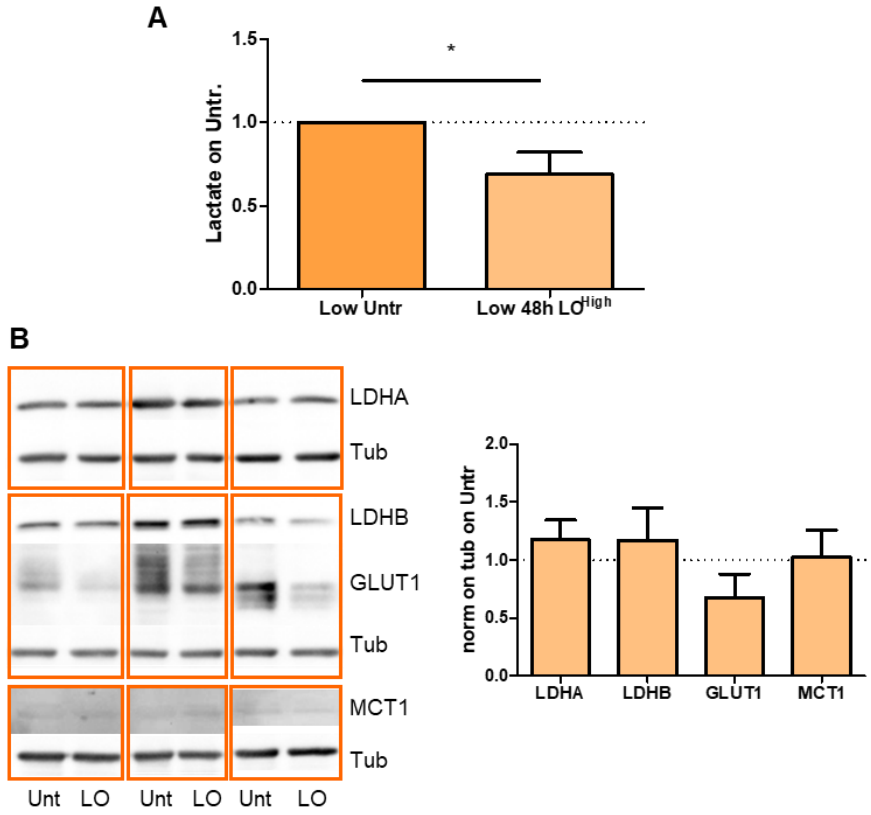

Fig.25 LO co-culture modifies metabolic behaviour of Low-V1G1 NS

(A) Extracellular lactate was evaluated after 48h of co-culture with LO isolated from High-V1G1 supernatant. (B) Metabolic enzymes (LDHA, LDHB, GLUT1 and MCT1) were evaluated by western blot, loading 40µg of proteins from total cell lysate. β-tubulin were used as normalizers and co-cultured samples were normalized on untreated. Statistic: Mann-Whitney t-test. A p=0.014

5.DISCUSSION

Our data show that High-V1G1 NS have higher lysosomal acidification, invasiveness, clonogenicity and ability to grow *in vivo* compared with NS with low expression of V-ATPase G1. High level of V1G1 subunit correlates with activation of ERK pathway.

The use of the V-ATPase specific inhibitor BafilomycinA1 (BafA1), reduces phospho-ERK level as well as other MAPK-correlated proteins such as CREB, GSK3a/b, MKK3, MKK6 and JNK2. Functionally, the activation of the V-ATPase-ERK interplay increases cell proliferation, cell cycle progression, motility and survival [82–85].

These phenotypes are abrogated only after BafA1 treatment, while the incubation of NS with inhibitors of lysosomal acidification (NH_4Cl) or ERK phosphorylation (PD98059) causes a milder effect.

High-V1G1 and Low-V1G1 NS are differentially sensitive to BafA1 treatment, with a stronger response observed in High-V1G1 NS. On the contrary, BafA1 modulates the autophagic flux (a signalling known to be induced by V-ATPase inhibition [91,92]) only in Low-V1G1 NS, whereas the autophagy marker p62 is poorly expressed in High-V1G1 NS and are not increased by BafA1.

This first set of data suggests that i) V-ATPase is crucial for NS homeostasis when is overexpressed and that these effects are achieved, at least in part, through ERK activation, ii) V-ATPase might play other functions in NS rather than regulating lysosomal acidification and autophagosome formation.

Therefore, we searched if V-ATPase was present on other organelles rather than the endo-lysosomal system, and if it could

sustain NS tumorigenesis through perturbation of the organelle homeostasis.

We observed that High-V1G1 NS had a more motile phenotype and this was reduced by BafA1 treatment. Since it was reported that mitochondria homeostasis is involved in cell motility and migration [93], we analysed whether V-ATPase G1 is present on these organelles.

Our preliminary data from super resolution imaging analysis, suggest that V1G1 subunit is localized at the mitochondria in NS.

Mitochondria are crucial organelles that play multiple roles, with regulation of cell bioenergetics be the most prominent [94]. In addition to energy production, they are involved in biosynthesis of macromolecules, regulation of cell death, Ca^{2+} homeostasis and cellular senescence [94,95].

Cell stress leads to the increase of ROS levels that facilitates the expression of pro-apoptotic genes and cytochrome c release from mitochondria, triggering apoptosis [94,96].

In this context our results show that BafA1 treatment causes depolarization of mitochondria and perturbs mitochondrial integral proteins expression only in High-V1G1 NS.

Furthermore, BafA1 induces ROS-mediated apoptosis, in a reversible way. Conversely, ERK inhibition or lysosome acidification impairment does not. Again, the two NS populations behave differently, with Low-V1G1 NS showing no increase in ROS levels or in the apoptotic fraction.

Despite we cannot conclude on a pathological model centred on mitochondrial V-ATPase, we can speculate about two possible

models involving V-ATPase and the organelle. In the first hypothesis, which we will refer at as “direct model” (Fig26A), in High-V1G1 NS the pump is localized not only on lysosomes, but also on mitochondria where it could co-operate to their polarization through the charges’ balance, maintaining a more negative matrix and a more positive intermembrane space. In the second hypothesis, the “indirect model” (Fig. 26B), mitochondria are affected by V-ATPase in an indirect way by contact with lysosomes or endosomes. Different organelles can make physical contacts and can communicate to exchange information and metabolites, so alteration in the activity of one organelle may reflect the stress of the other [97]. The most known of these contacts is the association of endoplasmic reticulum and mitochondria, but there is evidence of physical interaction between lysosomes and mitochondria too, for lipids or ions exchange [97–99]. According to this model, V-ATPase inhibition causes an impairment of lysosomes and a reduction of ions flux, as Ca^{2+}, from this organelle to mitochondrion, provoking charges unbalancing. This is followed by loss of mitochondria homeostasis in High-V1G1 NS, more sensitive to BafA1 treatment.

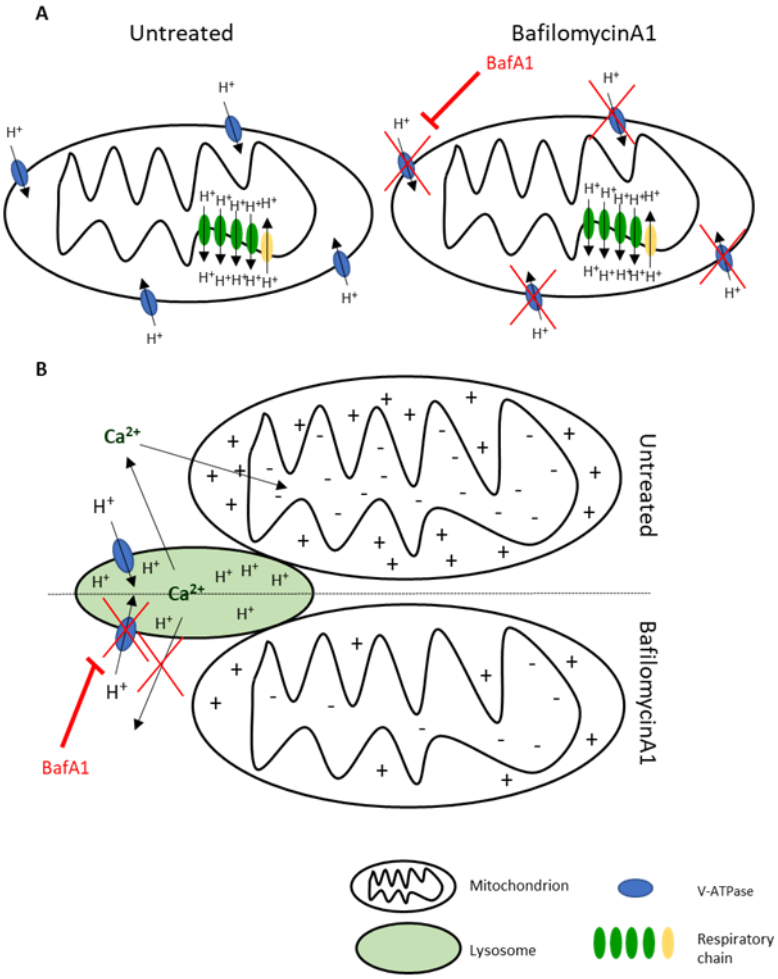

Fig.26: V-ATPase inhibition affects mitochondria homeostasis in High-V1G1 NS

(A) 1st hypothesis: direct effect of V-ATPase on mitochondria. V-ATPase inhibition causes an impairment of mitochondrion due to the localization of the proton pump on the organelle.

(B) 2nd hypothesis: indirect effect of V-ATPase on mitochondria due to the functional connection between lysosomes and mitochondria. Inhibition of lysosome activity provokes an unbalance of ions that affects charges in organelles, resulting in a mitochondria depolarization or damage.

Cancer cells are able to reprogram their metabolism, obtaining nutrients from a nutrient-poor environment: they deregulate the uptake of glucose and of amino acids and use glycolysis/TCA cycle molecules for biosynthesis [100].

In addition to the characterization of tumorigenic aspects and because of the central role of mitochondria in cell bioenergetics, we also investigated metabolic behaviors of High and Low-V1G1 NS.

In Low-V1G1 NS, the higher lactate production and higher level of LDHA enzyme, which produces lactate from pyruvate, suggests that their metabolism relies on glycolysis (Fig.27A, in red). This observation is line with the typical behaviour of cancer cells that generate lactate from glucose by fermentation even in presence of oxygen for rapid energy generation [101].

On the contrary, High-V1G1 NS use an oxidative metabolism, as showed by higher LDHB level, the enzyme, that converts lactate into pyruvate, suggesting that this cell population might use lactate as source of energy (Fig.27B in red), as previously described in other aggressive cancer cell types [102]. Finally, metabolic behaviour on High-V1G1 NS is reverted to the glycolytic one in presence of BafilomycinA1 treatment whereas aerobic glycolysis of Low-V1G1 NS is impaired when these cells are co-cultured with large oncosome vesicles secreted by High-V1G1 NS (Fig.27C and D, in red).

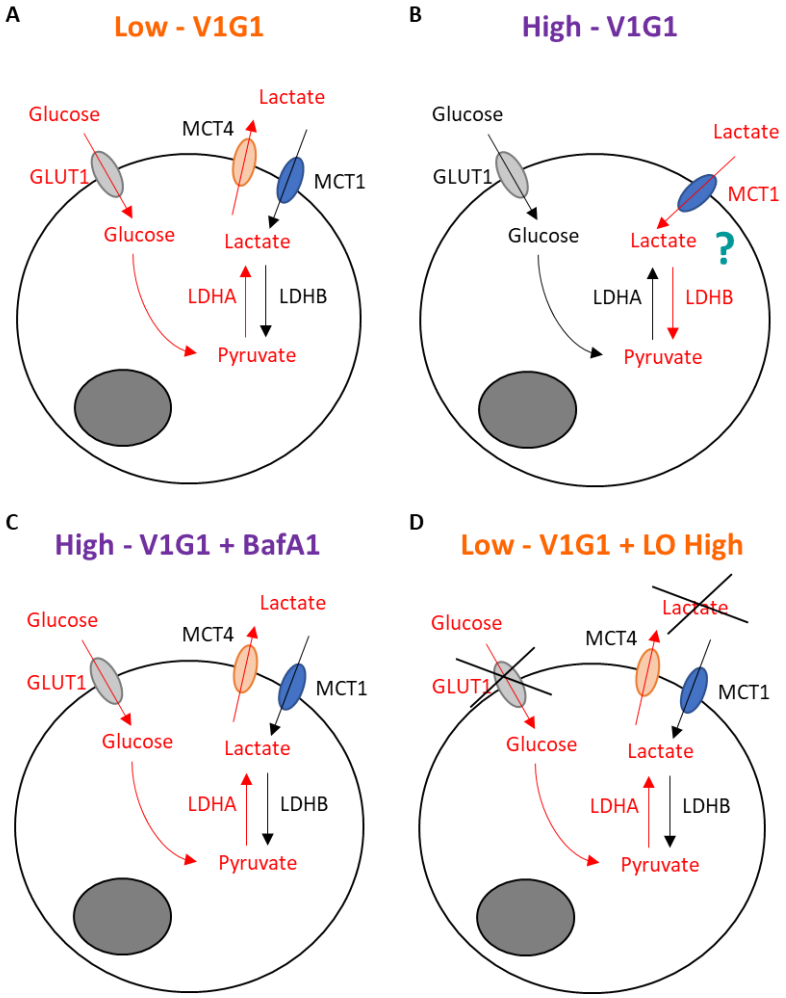

Fig.27: Metabolic behavior of High and Low-V1G1 NS

(A) Higher lactate production, higher LDHA level, lower extracellular glucose level and lower intracellular ATP suggest glycolytic metabolism in Low-V1G1 NS (aerobic glycolysis). (B) Higher intracellular ATP, higher extracellular glucose and higher LDHB suggest the use of oxidative metabolism by High-V1G1 NS (lactate consumption). (C) BafA1 treatment shifts metabolic behaviour of High-V1G1 to Low-V1G1 like metabolism, with the slight increase of lactate production and the slight increase of LDHA level. (D) Decrease of lactate production and slight decrease of GLUT1 indicate a reduction of aerobic glycolysis after LO co/culture in Low-V1G1 NS.

These data, although preliminary, indicate that the V-ATPase proton pump has a role in the regulation of GBM stem cells bioenergetics affecting mitochondria polarity and cellular metabolism in a dynamic fashion.

These results need to be confirmed at cellular level, to better elucidate the involvement of V-ATPase in modulating tumor phenotypes of the GBM stem cell niche.

Nevertheless, it is challenging to discriminate mitochondria proteins from lysosomal ones because the process of mitochondria isolation does not allow to purify mitochondria fraction from lysosomes, therefore resulting in lysosomal proteins contamination, including V-ATPase subunits. This caveat hinders our conclusion on V1G1 subcellular localization.

Furthermore, we will use broader strategies to better elucidate the role of V-ATPase modulation in GBM stem cells metabolism taking advantage of mass spectrometry to analyse the intra- and extra-cellular metabolOME, looking at gene expression level to understand which are the pathways correlated to the pump activity or after BafA1 or LO treatments and, finally, using a live-cell metabolic assay platform

6.CONCLUSIONS

In this thesis we provide further insights into the multiple roles played by V-ATPase to sustain glioma stem cell (GSC) viability looking at cell bioenergetics. We expand on our previous observation that GSC with higher levels of V1G1 subunit are characterized by a more aggressive phenotype providing in vivo evidence and we identify ERK as a preferential signalling activated in High-V1G1 cells. Furthermore, we provide initial evidence that pro-tumorigenic effects of V-ATPase are only partly related to lysosome function or ERK pathway activation. Other factors are involved in the V-ATPase directed signalling in glioma cells, such as mitochondrial homeostasis and cellular metabolism. Interestingly, we show that also the large extracellular vesicles produced by GSC are able to vehiculate V-ATPase subunits and to alter cellular metabolism of recipient cells to the state detected in High-V1G1 GSC. On the contrary, cellular bioenergetics are restored to “Low-V1G1 situation” when the pump activity is abrogated.

Given these data, we can conclude that V-ATPase plays a central role in cellular and metabolic signalling of glioma stem cells. Further studies are needed to confirm these results.

7.BIBLIOGRAPHY

[1] Bhavya B, Anand CR, Madhusoodanan UK, Rajalakshmi P, Krishnakumar K, Easwer H V., et al. To be Wild or Mutant: Role of Isocitrate Dehydrogenase 1 (IDH1) and 2-Hydroxy Glutarate (2-HG) in Gliomagenesis and Treatment Outcome in Glioma. Cell Mol Neurobiol 2019;1. doi:10.1007/s10571-019-00730-3.

[2] Pisapia DJ. The Updated World Health Organization Glioma Classification: Cellular and Molecular Origins of Adult Infiltrating Gliomas. Arch Pathol Lab Med 2017;141:1633–45. doi:10.5858/arpa.2016-0493-RA.

[3] Cohen-Inbar O. Geriatric brain tumor management part I: Meningioma. J Clin Neurosci 2019;67:5–9. doi:10.1016/j.jocn.2019.05.063.

[4] Ostrom QT, Gittleman H, Fulop J, Liu M, Blanda R, Kromer C, et al. CBTRUS Statistical Report: Primary Brain and Central Nervous System Tumors Diagnosed in the United States in 2008-2012. Neuro Oncol 2015;17:iv1–62. doi:10.1093/neuonc/nov189.

[5] Verhaak RGW, Hoadley KA, Purdom E, Wang V, Qi Y, Wilkerson MD, et al. Integrated Genomic Analysis Identifies Clinically Relevant Subtypes of Glioblastoma Characterized by Abnormalities in PDGFRA, IDH1, EGFR, and NF1. Cancer Cell 2010;17:98–110. doi:10.1016/j.ccr.2009.12.020.

[6] Ramirez Y, Weatherbee J, Wheelhouse R, Ross A. Glioblastoma Multiforme Therapy and Mechanisms of Resistance. Pharmaceuticals 2013;6:1475–506. doi:10.3390/ph6121475.

[7] Holland E, Ene C. Personalized Medicine for Gliomas. Surg Neurol Int 2015;6:89. doi:10.4103/2152-7806.151351.

[8] Xie Q, Mittal S, Berens ME. Targeting adaptive glioblastoma: an overview of proliferation and invasion. Neuro Oncol 2014;16:1575–84. doi:10.1093/neuonc/nou147.

[9] Singh SK, Hawkins C, Clarke ID, Squire JA, Bayani J, Hide T, et al. Identification of human brain tumour initiating cells. Nature 2004;432:396–401. doi:10.1038/nature03128.

[10] Gimple RC, Bhargava S, Dixit D, Rich JN. Glioblastoma stem cells: lessons from the tumor hierarchy in a lethal cancer. Genes Dev 2019;33:591–609. doi:10.1101/gad.324301.119.

[11] Cheng L, Huang Z, Zhou W, Wu Q, Donnola S, Liu JK, et al. Glioblastoma Stem Cells Generate Vascular Pericytes to Support Vessel Function and Tumor Growth. Cell 2013;153:139–52. doi:10.1016/j.cell.2013.02.021.

[12] Barnes JM, Kaushik S, Bainer RO, Sa JK, Woods EC, Kai F, et al. A tension-mediated glycocalyx–integrin feedback loop promotes mesenchymal-like glioblastoma. Nat Cell Biol 2018;20:1203–14.

doi:10.1038/s41556-018-0183-3.
[13] Shi Y, Ping Y-F, Zhou W, He Z-C, Chen C, Bian B-S-J, et al. Tumour-associated macrophages secrete pleiotrophin to promote PTPRZ1 signalling in glioblastoma stem cells for tumour growth. Nat Commun 2017;8:15080. doi:10.1038/ncomms15080.
[14] Zhang Y, Yu G, Chu H, Wang X, Xiong L, Cai G, et al. Macrophage-Associated PGK1 Phosphorylation Promotes Aerobic Glycolysis and Tumorigenesis. Mol Cell 2018;71:201-215.e7. doi:10.1016/j.molcel.2018.06.023.
[15] Alvarado AG, Thiagarajan PS, Mulkearns-Hubert EE, Silver DJ, Hale JS, Alban TJ, et al. Glioblastoma Cancer Stem Cells Evade Innate Immune Suppression of Self-Renewal through Reduced TLR4 Expression. Cell Stem Cell 2017;20:450-461.e4. doi:10.1016/j.stem.2016.12.001.
[16] Mooney J, Bernstock JD, Ilyas A, Ibrahim A, Yamashita D, Markert JM, et al. Current Approaches and Challenges in the Molecular Therapeutic Targeting of Glioblastoma. World Neurosurg 2019;129:90–100. doi:10.1016/j.wneu.2019.05.205.
[17] Stupp R, Mason WP, van den Bent MJ. “Radiotherapy plus Concomitant and Adjuvant Temozolomide for Glioblastoma.” Oncol Times 2005;27:15–6. doi:10.1097/01.COT.0000289242.47980.f9.
[18] Cohen MH, Shen YL, Keegan P, Pazdur R. FDA Drug Approval Summary: Bevacizumab (Avastin®) as Treatment of Recurrent Glioblastoma Multiforme. Oncologist 2012;17:1482–1482. doi:10.1634/theoncologist.2009-0121erratum.
[19] Messaoudi K, Clavreul A, Lagarce F. Toward an effective strategy in glioblastoma treatment. Part I: resistance mechanisms and strategies to overcome resistance of glioblastoma to temozolomide. Drug Discov Today 2015;20:899–905. doi:10.1016/j.drudis.2015.02.011.
[20] Selby MJ, Engelhardt JJ, Quigley M, Henning KA, Chen T, Srinivasan M, et al. Anti-CTLA-4 Antibodies of IgG2a Isotype Enhance Antitumor Activity through Reduction of Intratumoral Regulatory T Cells. Cancer Immunol Res 2013;1:32–42. doi:10.1158/2326-6066.CIR-13-0013.
[21] Zeng J, See AP, Phallen J, Jackson CM, Belcaid Z, Ruzevick J, et al. Anti-PD-1 Blockade and Stereotactic Radiation Produce Long-Term Survival in Mice With Intracranial Gliomas. Int J Radiat Oncol 2013;86:343–9. doi:10.1016/j.ijrobp.2012.12.025.
[22] Choi BD, Maus M V., June CH, Sampson JH. Immunotherapy for Glioblastoma: Adoptive T-cell Strategies. Clin Cancer Res 2019;25:2042–8. doi:10.1158/1078-0432.CCR-18-1625.
[23] Xu Q, Liu G, Yuan X, Xu M, Wang H, Ji J, et al. Antigen-Specific T-Cell Response from Dendritic Cell Vaccination Using Cancer Stem-

Like Cell-Associated Antigens. Stem Cells 2009;27:1734–40. doi:10.1002/stem.102.
[24] Benencia F, Courrèges MC, Fraser NW, Coukos G. Herpes virus oncolytic therapy reverses tumor immune dysfunction and facilitates tumor antigen presentation. Cancer Biol Ther 2008;7:1194–205. doi:10.4161/cbt.7.8.6216.
[25] Bejarano L, Schuhmacher AJ, Méndez M, Megías D, Blanco-Aparicio C, Martínez S, et al. Inhibition of TRF1 Telomere Protein Impairs Tumor Initiation and Progression in Glioblastoma Mouse Models and Patient-Derived Xenografts. Cancer Cell 2017;32:590-607.e4. doi:10.1016/j.ccell.2017.10.006.
[26] Sulli G, Rommel A, Wang X, Kolar MJ, Puca F, Saghatelian A, et al. Pharmacological activation of REV-ERBs is lethal in cancer and oncogene-induced senescence. Nature 2018;553:351–5. doi:10.1038/nature25170.
[27] Di Cristofori A, Ferrero S, Bertolini I, Gaudioso G, Russo MV, Berno V, et al. The vacuolar H+ ATPase is a novel therapeutic target for glioblastoma. Oncotarget 2015;6. doi:10.18632/oncotarget.4239.
[28] Stransky L, Cotter K, Forgac M. The Function of V-ATPases in Cancer. Physiol Rev 2016;96:1071–91. doi:10.1152/physrev.00035.2015.
[29] Forgac M. Vacuolar ATPases: rotary proton pumps in physiology and pathophysiology. Nat Rev Mol Cell Biol 2007;8:917–29. doi:10.1038/nrm2272.
[30] Yoshimori T, Yamamoto A, Moriyama Y, Futai M, Tashiro Y. Bafilomycin A1, a specific inhibitor of vacuolar-type H(+)-ATPase, inhibits acidification and protein degradation in lysosomes of cultured cells. J Biol Chem 1991;266:17707–12.
[31] Pamarthy S, Kulshrestha A, Katara GK, Beaman KD. The curious case of vacuolar ATPase: regulation of signaling pathways. Mol Cancer 2018;17:41. doi:10.1186/s12943-018-0811-3.
[32] Nishi T, Forgac M. The vacuolar (H+)-ATPases — nature's most versatile proton pumps. Nat Rev Mol Cell Biol 2002;3:94–103. doi:10.1038/nrm729.
[33] Toei M, Saum R, Forgac M. Regulation and Isoform Function of the V-ATPases. Biochemistry 2010;49:4715–23. doi:10.1021/bi100397s.
[34] Cotter K, Stransky L, McGuire C, Forgac M. Recent Insights into the Structure, Regulation, and Function of the V-ATPases. Trends Biochem Sci 2015;40:611–22. doi:10.1016/j.tibs.2015.08.005.
[35] Yu Z, Zhao L-X, Jiang C-L, Duan Y, Wong L, Carver KC, et al. Bafilomycins produced by an endophytic actinomycete Streptomyces sp. YIM56209. J Antibiot (Tokyo) 2011;64:159–62. doi:10.1038/ja.2010.147.
[36] Werner G, Hagenmaier H, Drautz H, Baumgartner A, ZÄHNER H.

Metabolic products of microorganisms. 224. Bafilomycins, a new group of macrolide antibiotics. Production, isolation, chemical structure and biological activity. J Antibiot (Tokyo) 1984;37:110–7. doi:10.7164/antibiotics.37.110.
[37] Wilton JH, Hokanson GC, French JC. PD 118,576: A new antitumor macrolide antibiotic. J Antibiot (Tokyo) 1985;38:1449–52. doi:10.7164/antibiotics.38.1449.
[38] Frändberg E, Petersson C, Lundgren LN, Schnürer J. Streptomyces halstedii K122 produces the antifungal compounds bafilomycin B1 and C1. Can J Microbiol 2000;46:753–8.
[39] Vaněk Z, Matějů J, Čurdová E. Immunomodulators isolated from microorganisms. Folia Microbiol (Praha) 1991;36:99–111. doi:10.1007/BF02814487.
[40] Goetz MA, McCormick PA, Monaghan RL, Ostlind DA, Hensens OD, Liesch JM, et al. L-155,175: A new antiparasitic macrolide fermentation, isolation and structure. J Antibiot (Tokyo) 1985;38:161–8. doi:10.7164/antibiotics.38.161.
[41] Bowman EJ, Siebers A, Altendorf K. Bafilomycins: a class of inhibitors of membrane ATPases from microorganisms, animal cells, and plant cells. Proc Natl Acad Sci 1988;85:7972–6. doi:10.1073/pnas.85.21.7972.
[42] Whitton B, Okamoto H, Packham G, Crabb SJ. Vacuolar ATPase as a potential therapeutic target and mediator of treatment resistance in cancer. Cancer Med 2018;7:3800–11. doi:10.1002/cam4.1594.
[43] Saftig P, Klumperman J. Lysosome biogenesis and lysosomal membrane proteins: trafficking meets function. Nat Rev Mol Cell Biol 2009;10:623–35. doi:10.1038/nrm2745.
[44] Scott CC, Gruenberg J. Ion flux and the function of endosomes and lysosomes: pH is just the start. BioEssays 2011;33:103–10. doi:10.1002/bies.201000108.
[45] Sachse M, Ramm G, Strous G, Klumperman J. Endosomes: multipurpose designs for integrating housekeeping and specialized tasks. Histochem Cell Biol 2002;117:91–104. doi:10.1007/s00418-001-0348-0.
[46] Boecker CA, Holzbaur EL. Vesicular degradation pathways in neurons: at the crossroads of autophagy and endo-lysosomal degradation. Curr Opin Neurobiol 2019;57:94–101. doi:10.1016/j.conb.2019.01.005.
[47] Baron M. Endocytic routes to Notch activation. Semin Cell Dev Biol 2012;23:437–42. doi:10.1016/j.semcdb.2012.01.008.
[48] Cruciat C-M, Ohkawara B, Acebron SP, Karaulanov E, Reinhard C, Ingelfinger D, et al. Requirement of Prorenin Receptor and Vacuolar H+-ATPase-Mediated Acidification for Wnt Signaling. Science (80-) 2010;327:459–63. doi:10.1126/science.1179802.

[49] Valapala M, Hose S, Gongora C, Dong L, Wawrousek EF, Samuel Zigler J, et al. Impaired endolysosomal function disrupts Notch signalling in optic nerve astrocytes. Nat Commun 2013;4:1629. doi:10.1038/ncomms2624.
[50] Sethi N, Yan Y, Quek D, Schupbach T, Kang Y. Rabconnectin-3 Is a Functional Regulator of Mammalian Notch Signaling. J Biol Chem 2010;285:34757–64. doi:10.1074/jbc.M110.158634.
[51] Peña-Llopis S, Vega-Rubin-de-Celis S, Schwartz JC, Wolff NC, Tran TAT, Zou L, et al. Regulation of TFEB and V-ATPases by mTORC1. EMBO J 2011;30:3242–58. doi:10.1038/emboj.2011.257.
[52] Williamson WR, Hiesinger PR. On the role of v-ATPase V0a1–dependent degradation in Alzheimer Disease. Commun Integr Biol 2010;3:604–7. doi:10.4161/cib.3.6.13364.
[53] Kornak U, Reynders E, Dimopoulou A, van Reeuwijk J, Fischer B, Rajab A, et al. Impaired glycosylation and cutis laxa caused by mutations in the vesicular H+-ATPase subunit ATP6V0A2. Nat Genet 2008;40:32–4. doi:10.1038/ng.2007.45.
[54] Wagner CA, Finberg KE, Breton S, Marshansky V, Brown D, Geibel JP. Renal Vacuolar H + -ATPase. Physiol Rev 2004;84:1263–314. doi:10.1152/physrev.00045.2003.
[55] Toyomura T, Murata Y, Yamamoto A, Oka T, Sun-Wada G-H, Wada Y, et al. From Lysosomes to the Plasma Membrane. J Biol Chem 2003;278:22023–30. doi:10.1074/jbc.M302436200.
[56] Pietrement C, Sun-Wada G-H, Da Silva N, McKee M, Marshansky V, Brown D, et al. Distinct Expression Patterns of Different Subunit Isoforms of the V-ATPase in the Rat Epididymis1. Biol Reprod 2006;74:185–94. doi:10.1095/biolreprod.105.043752.
[57] McConnell M, Feng S, Chen W, Zhu G, Shen D, Ponnazhagan S, et al. Osteoclast proton pump regulator Atp6v1c1 enhances breast cancer growth by activating the mTORC1 pathway and bone metastasis by increasing V-ATPase activity. Oncotarget 2017;8. doi:10.18632/oncotarget.17544.
[58] Son SW, Kim S-H, Moon E-Y, Kim D-H, Pyo S, Um SH. Prognostic significance and function of the vacuolar H^+-ATPase subunit V1E1 in esophageal squamous cell carcinoma. Oncotarget 2016;7:49334–48. doi:10.18632/oncotarget.10340.
[59] Liu P, Chen H, Han L, Zou X, Shen W. Expression and role of V1A subunit of V-ATPases in gastric cancer cells. Int J Clin Oncol 2015;20:725–35. doi:10.1007/s10147-015-0782-y.
[60] Cotter K, Capecci J, Sennoune S, Huss M, Maier M, Martinez-Zaguilan R, et al. Activity of Plasma Membrane V-ATPases Is Critical for the Invasion of MDA-MB231 Breast Cancer Cells. J Biol Chem 2015;290:3680–92. doi:10.1074/jbc.M114.611210.
[61] Lu Q, Lu S, Huang L, Wang T, Wan Y, Zhou CX, et al. The

expression of V-ATPase is associated with drug resistance and pathology of non-small-cell lung cancer. Diagn Pathol 2013;8:824. doi:10.1186/1746-1596-8-145.
[62] Nishisho T, Hata K, Nakanishi M, Morita Y, Sun-Wada G-H, Wada Y, et al. The a3 Isoform Vacuolar Type H+-ATPase Promotes Distant Metastasis in the Mouse B16 Melanoma Cells. Mol Cancer Res 2011;9:845–55. doi:10.1158/1541-7786.MCR-10-0449.
[63] Xu J, Xie R, Liu X, Wen G, Jin H, Yu Z, et al. Expression and functional role of vacuolar H+-ATPase in human hepatocellular carcinoma. Carcinogenesis 2012;33:2432–40. doi:10.1093/carcin/bgs277.
[64] Katara GK, Kulshrestha A, Mao L, Wang X, Sahoo M, Ibrahim S, et al. Mammary epithelium-specific inactivation of V-ATPase reduces stiffness of extracellular matrix and enhances metastasis of breast cancer. Mol Oncol 2018;12:208–23. doi:10.1002/1878-0261.12159.
[65] Kulshrestha A, Katara GK, Ibrahim S, Pamarthy S, Jaiswal MK, Sachs AG, et al. Vacuolar ATPase 'a2' isoform exhibits distinct cell surface accumulation and modulates matrix metalloproteinase activity in ovarian cancer. Oncotarget 2015;6. doi:10.18632/oncotarget.2902.
[66] Michel V, Licon-Munoz Y, Trujillo K, Bisoffi M, Parra KJ. Inhibitors of vacuolar ATPase proton pumps inhibit human prostate cancer cell invasion and prostate-specific antigen expression and secretion. Int J Cancer 2013;132:E1–10. doi:10.1002/ijc.27811.
[67] Bunney PE, Zink AN, Holm AA, Billington CJ, Kotz CM. Orexin activation counteracts decreases in nonexercise activity thermogenesis (NEAT) caused by high-fat diet. Physiol Behav 2017;176:139–48. doi:10.1016/j.physbeh.2017.03.040.
[68] Huang L, Lu Q, Han Y, Li Z, Zhang Z, Li X. ABCG2/V-ATPase was associated with the drug resistance and tumor metastasis of esophageal squamous cancer cells. Diagn Pathol 2012;7:180. doi:10.1186/1746-1596-7-180.
[69] Feng S, Cai M, Liu P, Wei L, Wang J, Qi J, et al. Atp6v1c1 May Regulate Filament Actin Arrangement in Breast Cancer Cells. PLoS One 2014;9:e84833. doi:10.1371/journal.pone.0084833.
[70] Wojtkowiak JW, Verduzco D, Schramm KJ, Gillies RJ. Drug Resistance and Cellular Adaptation to Tumor Acidic pH Microenvironment. Mol Pharm 2011;8:2032–8. doi:10.1021/mp200292c.
[71] Sennoune SR, Martinez-Zaguilan R. Plasmalemmal vacuolar H+-ATPases in angiogenesis, diabetes and cancer. J Bioenerg Biomembr 2007;39:427–33. doi:10.1007/s10863-007-9108-8.
[72] Tschan MP, Simon H-U. The role of autophagy in anticancer therapy: promises and uncertainties. J Intern Med 2010;268:410–8.

doi:10.1111/j.1365-2796.2010.02266.x.
[73] Mathew R, Karp CM, Beaudoin B, Vuong N, Chen G, Chen H-Y, et al. Autophagy Suppresses Tumorigenesis through Elimination of p62. Cell 2009;137:1062–75. doi:10.1016/j.cell.2009.03.048.
[74] Terrasi A, Bertolini I, Martelli C, Gaudioso G, Di Cristofori A, Storaci AM, et al. Specific V-ATPase expression sub-classifies IDHwt lower-grade gliomas and impacts glioma growth in vivo. EBioMedicine 2019;41:214–24. doi:10.1016/j.ebiom.2019.01.052.
[75] Bertolini I, Terrasi A, Martelli C, Gaudioso G, Di Cristofori A, Storaci AM, et al. A GBM-like V-ATPase signature directs cell-cell tumor signaling and reprogramming via large oncosomes. EBioMedicine 2019;41:225–35. doi:10.1016/j.ebiom.2019.01.051.
[76] Minciacchi VR, You S, Spinelli C, Morley S, Zandian M, Aspuria P-J, et al. Large oncosomes contain distinct protein cargo and represent a separate functional class of tumor-derived extracellular vesicles. Oncotarget 2015;6:11327–41. doi:10.18632/oncotarget.3598.
[77] Vinod V, Padmakrishnan CJ, Vijayan B, Gopala S. 'How can I halt thee?' The puzzles involved in autophagic inhibition. Pharmacol Res 2014;82:1–8. doi:10.1016/j.phrs.2014.03.005.
[78] Alessi DR, Cuenda A, Cohen P, Dudley DT, Saltiel AR. PD 098059 Is a Specific Inhibitor of the Activation of Mitogen-activated Protein Kinase Kinase in Vitro and in Vivo. J Biol Chem 1995;270:27489–94. doi:10.1074/jbc.270.46.27489.
[79] Settembre C, Fraldi A, Medina DL, Ballabio A. Signals from the lysosome: a control centre for cellular clearance and energy metabolism. Nat Rev Mol Cell Biol 2013;14:283–96. doi:10.1038/nrm3565.
[80] Natsumeda M, Maitani K, Liu Y, Miyahara H, Kaur H, Chu Q, et al. Targeting Notch Signaling and Autophagy Increases Cytotoxicity in Glioblastoma Neurospheres. Brain Pathol 2016;26:713–23. doi:10.1111/bpa.12343.
[81] Muniraj N, Siddharth S, Nagalingam A, Walker A, Woo J, Győrffy B, et al. Withaferin A inhibits lysosomal activity to block autophagic flux and induces apoptosis via energetic impairment in breast cancer cells. Carcinogenesis 2019:1–11. doi:10.1093/carcin/bgz015.
[82] Chen F. JNK-Induced Apoptosis, Compensatory Growth, and Cancer Stem Cells. Cancer Res 2012;72:379–86. doi:10.1158/0008-5472.CAN-11-1982.
[83] Fan S, Wang Y, Lu J, Zheng Y, Wu D, Zhang Z, et al. CERS2 Suppresses Tumor Cell Invasion and is Associated with Decreased V-ATPase and MMP-2/MMP-9 Activities in Breast Cancer. J Cell Biochem 2015;116:502–13. doi:10.1002/jcb.24978.
[84] De Luca A, Maiello MR, D'Alessio A, Pergameno M, Normanno N. The RAS/RAF/MEK/ERK and the PI3K/AKT signalling pathways:

role in cancer pathogenesis and implications for therapeutic approaches. Expert Opin Ther Targets 2012;16:S17–27. doi:10.1517/14728222.2011.639361.
[85] Mancinelli R, Carpino G, Petrungaro S, Mammola CL, Tomaipitinca L, Filippini A, et al. Multifaceted Roles of GSK-3 in Cancer and Autophagy-Related Diseases. Oxid Med Cell Longev 2017;2017:1–14. doi:10.1155/2017/4629495.
[86] Zheng KB, Xie J, Li YT, Yuan Y, Wang Y, Li C, et al. Knockdown of CERB expression inhibits proliferation and migration of glioma cells line U251. Bratislava Med J 2019;120:309–15. doi:10.4149/BLL_2019_049.
[87] Zhao H, Halicka HD, Li J, Biela E, Berniak K, Dobrucki J, et al. DNA damage signaling, impairment of cell cycle progression, and apoptosis triggered by 5-ethynyl-2′-deoxyuridine incorporated into DNA. Cytom Part A 2013;83:979–88. doi:10.1002/cyto.a.22396.
[88] Anada T, Fukuda J, Sai Y, Suzuki O. An oxygen-permeable spheroid culture system for the prevention of central hypoxia and necrosis of spheroids. Biomaterials 2012;33:8430–41. doi:10.1016/j.biomaterials.2012.08.040.
[89] Hirschhaeuser F, Menne H, Dittfeld C, West J, Mueller-Klieser W, Kunz-Schughart LA. Multicellular tumor spheroids: An underestimated tool is catching up again. J Biotechnol 2010;148:3–15. doi:10.1016/j.jbiotec.2010.01.012.
[90] Naviglio S. Lactic dehydrogenase and cancer an overview. Front Biosci 2015;20:4368. doi:10.2741/4368.
[91] Nagelkerke A, Bussink J, Geurts-Moespot A, Sweep FCGJ, Span PN. Therapeutic targeting of autophagy in cancer. Part II: Pharmacological modulation of treatment-induced autophagy. Semin Cancer Biol 2015;31:99–105. doi:10.1016/j.semcancer.2014.06.001.
[92] Nagelkerke A, Sweep FCGJ, Geurts-Moespot A, Bussink J, Span PN. Therapeutic targeting of autophagy in cancer. Part I: Molecular pathways controlling autophagy. Semin Cancer Biol 2015;31:89–98. doi:10.1016/j.semcancer.2014.05.004.
[93] Rivadeneira DB, Caino MC, Seo JH, Angelin A, Wallace DC, Languino LR, et al. Survivin promotes oxidative phosphorylation, subcellular mitochondrial repositioning, and tumor cell invasion. Sci Signal 2015;8:ra80–ra80. doi:10.1126/scisignal.aab1624.
[94] Vakifahmetoglu-Norberg H, Ouchida AT, Norberg E. The role of mitochondria in metabolism and cell death. Biochem Biophys Res Commun 2017;482:426–31. doi:10.1016/j.bbrc.2016.11.088.
[95] Galluzzi L, Joza N, Tasdemir E, Maiuri MC, Hengartner M, Abrams JM, et al. No death without life: vital functions of apoptotic effectors. Cell Death Differ 2008;15:1113–23. doi:10.1038/cdd.2008.28.
[96] Zhou DR, Eid R, Boucher E, Miller KA, Mandato CA, Greenwood

MT. Stress is an agonist for the induction of programmed cell death: A review. Biochim Biophys Acta - Mol Cell Res 2019;1866:699–712. doi:10.1016/j.bbamcr.2018.12.001.
[97] Soto-Heredero G, Baixauli F, Mittelbrunn M. Interorganelle Communication between Mitochondria and the Endolysosomal System. Front Cell Dev Biol 2017;5:1–8. doi:10.3389/fcell.2017.00095.
[98] Todkar K, Ilamathi HS, Germain M. Mitochondria and Lysosomes: Discovering Bonds. Front Cell Dev Biol 2017;5:1–7. doi:10.3389/fcell.2017.00106.
[99] Wong YC, Ysselstein D, Krainc D. Mitochondria–lysosome contacts regulate mitochondrial fission via RAB7 GTP hydrolysis. Nature 2018;554:382–6. doi:10.1038/nature25486.
[100] Pavlova NN, Thompson CB. The Emerging Hallmarks of Cancer Metabolism. Cell Metab 2016;23:27–47. doi:10.1016/j.cmet.2015.12.006.
[101] Liberti M V, Locasale JW. The Warburg Effect: How Does it Benefit Cancer Cells? Trends Biochem Sci 2016;41:211–8. doi:10.1016/j.tibs.2015.12.001.
[102] Martínez-Reyes I, Chandel NS. Waste Not, Want Not: Lactate Oxidation Fuels the TCA Cycle. Cell Metab 2017;26:803–4. doi:10.1016/j.cmet.2017.11.005.

8.RESEARCH INTEGRITY DECLARATION:

Results reported in this work comply with the four fundamental principles of research integrity of The European Code of Conduct for Research Integrity (ALLEA - All European Academies, Berlin 2018; www.allea.org):

- Reliability in ensuring the quality of research, reflected in the design, the methodology, the analysis and the use of resources;
- Honesty in developing, undertaking, reviewing, reporting and communicating research in a transparent, fair, full and unbiased way;
- Respect for colleagues, research participants, society, ecosystems, cultural heritage and the environment;
- Accountability for the research from idea to publication, for its management and organization, for training, supervision and mentoring, and for its wider impacts.

9.SCIENTIFIC PRODUCTS

Poster:

- V-ATPase in glioma stem cells: V1G1 subunit expression correlates with metabolic behavior and mitochondria activity.
  Storaci A.M., Bertolini I., Caroli M., Ferrero S., Vaira V.
  AACR Annual Meeting 2019 - American Association for Cancer Research.
  Atlanta, March 29- 3 April 3rd, 2019 Atlanta Georgia

- V-ATPase activity in glioma stem cells: V1G1 expression determines sensitivity to BafilomycinA1 and subcellular localization of the pump.
  Storaci A.M., Bertolini I., Caroli M., Ferrero S., Vaira V.
  EACR 2018 - 25th Biennal Congress of the European Association for Cancer Research. Amsterdam, June 30 – July 3rd, 2018

- V-ATPase modulation & metabolic processes in glioma stem cells.
  Storaci A.M., Bertolini I., Di Cristofori A., Caroli M., Ferrero S., Vaira V.
  ISCaM 2017 – 4th Annual Meeting of the International Society of Cancer Metabolism. Bertinoro – October 19-21, 2017

Papers:

- MFF regulation of mitochondrial cell death is a therapeutic target in cancer.
  Seo JH, Chae YC, Kossenkov AV, Lee YG, Tang HY, Agarwal E, Gabrilovich DI, Languino LR, Speicher DW, Shastrula PK, Storaci AM, Ferrero S, Gaudioso G, Caroli M, Tosi D, Giroda M, Vaira V, Rebecca VW, Herlyn M, Xiao M, Fingerman D, Martorella A, Skordalakes E, Altieri DC.
  Cancer Res. 2019 doi: 10.1158/0008-5472.CAN-19-1982

- Mitochondrial fission factor is a novel Myc-dependent regulator of mitochondrial permeability in cancer.
  Seo JH, Agarwal E, Chae YC, Lee YG, Garlick DS, Storaci AM, Ferrero S, Gaudioso G, Gianelli U, Vaira V, Altieri DC.
  EBioMedicine. 2019 doi: 10.1016/j.ebiom.2019.09.017.

- A GBM-like V-ATPase signature directs cell-cell tumor signaling and reprogramming via large oncosomes.
  Bertolini I, Terrasi A, Martelli C, Gaudioso G, Di Cristofori A, Storaci AM, Formica M, Braidotti P, Todoerti K, Ferrero S, Caroli M, Ottobrini L, Vaccari T, Vaira v.
  EBioMedicine. 2019 doi: 10.1016/j.ebiom.2019.01.051.

- Specific V-ATPase expression sub-classifies IDHwt lower-grade gliomas and impacts glioma growth in vivo
  Terrasi A, Bertolini I, Martelli C, Gaudioso G, Di Cristofori A, Storaci AM, Formica M, Bosari S, Caroli M, Ottobrini L, Vaccari T, Vaira V.
  EBioMedicine. 2019 doi: 10.1016/j.ebiom.2019.01.052.

10.ACKNOWLEDGEMENTS

This work was supported by Fondazione Cariplo (2014-1148 to Valentina Vaira), Fondazione IRCCS Ca' Granda and Fondazione INGM Grant in Molecular Medicine (to Valentina Vaira) and by the Ricerca Corrente Program (to Stefano Ferrero).

For this work I want to thank my co-tutor, Dr. Valentina Vaira for the supervision during these 3 years of PhD; my tutor, Prof. Stefano Ferrero for the opportunity to work in molecular pathology lab; Dr. Irene Bertolini for sharing with me the project of V-ATPase role in glioma stem cells and to all the members of molecular pathology lab.

Thanks also to Dr. Manuela Caroli of Neurosurgery Unit of Fondazione IRCCS Ca' Granda Ospedale Maggiore Policlinico for providing patients' samples and to Dr. Maria Carla Panzeri of Alembic - San Raffaele for electron microscopy images.

This thesis was evaluated by 3 independent reviewers:

Prof. Dario C. Altieri M.D.
Professor in Cancer Biology
Immunology, Microenvironment and Metastasis Program.
The Wistar Institute, Philadelphia, PA 19104

Prof. Marialuisa Lavitrano
Professor in Pathology and Immunology
Department of Medicine and Surgery
University Milano-Bicocca, Milan

Prof. Rosa Maria Moresco
Professor in Applied Medical Technologies
Department of Medicine and Surgery
University Milano-Bicocca, Milan